

Brain-derived neurotrophic factor in platelet derived extracellular vesicles

The University of Helsinki
Faculty of Biological and Environmental
Sciences
Department of Biosciences
Pro gradu thesis
Biochemistry
December 2019
Anna-Emilia Lindelöf
Supervisors Pia Siljander
Mari Palviainen

Tiedekunta - Fakultet - Faculty Faculty of Biological and Environmental Sciences		Laitos - Institution - Department Department of Biosciences	
Tekijä - Författare - Author Anna-Emilia Lindelöf			
Title Brain-derived neurotrophic factor in platelet derived extracellular vesicles			
Oppiaine - Läroämne - Subject Biochemistry			
Työn laji/ Ohjaaja - Arbetets art/Handledare - Level/Instructor Pro gradu -thesis / Pia Siljander, Mari Palviainen,		Aika - Datum - Month and year December 2019	Sivumäärä - Sidoantal - Number of pages 64
<p>Tiivistelmä - Referat - Abstract</p> <p>Background. Platelets are known to contain ample amounts of brain derived neurotrophic factor. Previous spectrophotometric studies carried out in Pia Siljander's lab have shown that BDNF is secreted from activated platelets packed in extracellular vesicles. For this project we wanted to 1) confirm that BDNF really is secreted in extracellular vesicles (EVs) 2) find out how the choice of agonist affected the BDNF cargo of the platelet derived EVs, and 3) find out if the BDNF is packed into EVs of certain densities rather than others.</p> <p>Methods. The platelets were isolated from platelet concentrates by size exclusion chromatography. The isolated platelets were then activated by thrombin and collagen co-stimulation (TC) and by Ca^{2+} ionophore, respectively. The platelet activation produced extracellular vesicles (PEVs) which were isolated by differential ultracentrifugation. The isolated PEVs were then analysed by flow cytometry, ELISA and Western blot for EV typical membrane surface proteins and for their BDNF content. As we were interested finding out whether BDNF is enriched in PEVs to certain populations, density gradient centrifugation was performed. These samples were also analysed by Western blot and by ELISA. The size distribution and concentration of PEVs in all samples was analysed by Nanoparticle tracking analysis.</p> <p>Results and conclusions. This study confirmed that platelets secrete PEVs as a response to agonists. PEVs with higher BDNF concentration were produced using TC co-stimulation as compared to PEVs derived from the Ca^{2+} ionophore. The result implies that BDNF is actively packed into PEVs for instance as a thrombogenic response. Based on the density gradient results it seems that BDNF was packed into certain population of PEVs with a density between 1.112 g ml^{-1} and 1.132 g ml^{-1} corresponding to a particle diameter of less than 500 nm. The finding that BDNF is actively packed into TC co-stimulation derived PEVs of a certain population is interesting from a therapeutic point of view, since EVs are likely to be key players in the development of new cell-based therapies.</p> <p>Had there been more time, it would have been interesting to optimize both the density gradient protocol and the ELISA analysis. This optimization of methods would make the process more efficient, less prone to sample loss, not to mention that there would be less intra-assay variation.</p>			
<p>Keywords</p> <p>Brain derived neurotrophic factor, density gradient centrifugation, ELISA, extracellular vesicle, flow cytometry, nanoparticle tracking analysis, platelet, Western blot</p>			
Säilytyspaikka - Förvaringsställe - Where deposited			
Muita tietoja - Övriga uppgifter - Additional information			

Tiedekunta - Fakultet - Faculty Bio- och miljövetenskapliga fakulteten		Laitos - Institution - Department Institutionen för biovetenskaper	
Tekijä - Författare - Author Anna-Emilia Lindelöf			
Työn nimi - Arbetets titel Brain-derived neurotrophic factor i extracellulära vesiklar, som härstammar från blodplättar			
Oppiaine - Läroämne - Subject Biokemi			
Työn laji/ Ohjaaja - Arbetets art/Handledare - Level/Instructor Pro gradu- avhandling / Pia Siljander, Mari Palviainen		Aika - Datum - Month and year December 2019	Sivumäärä - Sidoantal - Number of pages 64
<p>Tiivistelmä - Referat - Abstract</p> <p>Bakgrund. Blodplättar innehåller stora mängder av proteinet brain-derived neurotrophic factor. På basen av tidigare spektrofotometriska studier, som utförts i Pia Siljanders laboratorium, vet vi att aktiverade blodplättar utsöndrar brain-derived neurotrophic factor packat i extracellulära vesiklar. Under detta projekt ville vi för det första, bekräfta att brain-derived neurotrophic factor utsöndras ur aktiverade blodplättar. För det andra, ville vi veta hur valet av agonist påverkar brain-derived neurotrophic factor -innehållet i de utsöndrade extracellulära vesiklarna. För det tredje, ville vi veta huruvida brain-derived neurotrophic factor selektivt packas i vissa populationer av extracellulära vesiklar.</p> <p>Metoder. Blodplättarna isolerades från blodplättskoncentrat med storleksseparationskromatografi. De isolerade blodplättarna aktiverades sedan med trombin och kollagen co-stimulation eller Ca^{2+} ionofor. Aktiveringen resulterade i extracellulära vesiklar, som härstammade från blodplättar. Dessa extracellulära vesiklar isolerades sedan genom differentiell ultracentrifugering. De isolerade extracellulära vesiklarna analyserades med flödescytometri, ELISA och Western blot för både EV-typiska membranproteiner och brain-derived neurotrophic factor. Då vi var intresserade av att få veta huruvida brain-derived neurotrophic factor berikas i specifika populationer av extracellulära vesiklar med ursprung i blodplättar utförde vi även gradientcentrifugering. Även dessa prover analyserades med ELISA och Western blot. Storleksdistributionen och koncentrationen av extracellulära vesiklar analyserades med nanoparticle tracking analysis</p> <p>Resultat och slutsatser. Vi fastställde att blodplättar utsöndrar extracellulära vesiklar då de behandlas med agonister. Då blodplättar stimulerades med trombin och kollagen co-stimulering resulterade det i extracellulära vesiklar med en högre koncentration brain-derived neurotrophic factor än då Ca^{2+} ionofor används som agonist. Resultaten tyder på att brain-derived neurotrophic factor aktivt och specifikt packas i bestämda populationer av extracellulära vesiklar. Detta kan exempelvis ske som en inflammatorisk respons. Enligt resultaten från gradientcentrifugeringen packas brain-derived neurotrophic factor i populationer av extracellulära vesiklar med en densitet mellan 1,112 g ml⁻¹ och 1132 g ml⁻¹. Dessa densiteter motsvarar en partikeldiameter under 500 nm. Faktum att brain-derived neurotrophic factor aktivt packas i extracellulära vesiklar, som härstammar från blodplättar, med viss densitet och diameter är ett intressant resultat till exempel ur en teragnostisk synvinkel, eftersom extracellulära vesiklar sannolikt är i nyckelroll då nya cellbaserade terapiformer utvecklas.</p> <p>Om det hade funnits mera tid hade det varit intressant att optimera metoden för både gradientcentrifugering och för ELISA. Då hade processen blivit mer effektiv och mindre utsatt för materialförlust. Dessutom skulle resultaten vara mer pålitliga i.o.m mindre variation inom analysen. Intressant vore också att pröva hur olika agonister påverkar koncentrationen brain-derived neurotrophic factor i extracellulära vesiklar, som härstammar från blodplättar. Faktumet att brain-derived neurotrophic factor aktivt packas i extracellulära vesiklar, som härstammar från blodplättar med viss densitet och diameter är ett intressant resultat till exempel ur en teragnostisk synvinkel, eftersom extracellulära vesiklar sannolikt är i nyckelroll då nya cellbaserade terapiformer utvecklas.</p>			

Avainsanat - Nyckelord

Blodplättar, brain-derived neurotrophic factor, densitets gradient, ELISA, extracellulära vesiklar
flödescytometri, nanoparticle tracking analysis, Western blot

Säilytyspaikka - Förvaringsställe - Where deposited

Muita tietoja - Övriga uppgifter - Additional information

Table of Contents

1. BACKGROUND.....	10
1.1 PLATELETS.....	10
1.2 BRAIN-DERIVED NEUROTROPHIC FACTOR	13
1.3 EXTRACELLULAR VESICLES	16
1.4 PLATELETS AND EXTRACELLULAR VESICLES	20
1.5 ISOLATING EXTRACELLULAR VESICLES.....	22
2. AIM OF THE PROJECT	24
3. MATERIALS AND METHODS.....	24
3.1 ISOLATION OF PLATELETS.....	24
3.2 ACTIVATION OF PLATELETS.....	26
3.3 ISOLATION OF PEVS	27
3.4 PLATELET AND EV FLOW CYTOMETRY	27
3.5 DENSITY-GRADIENT.....	27
3.5.1 APPLYING THE DENSITY-GRADIENT METHOD	29
3.6 DETERMINING THE SIZE DISTRIBUTION AND CONCENTRATION OF THE EV POPULATIONS.....	29
3.7 SDS-PAGE AND WESTERN BLOT.....	30
3.8 ELISA ANALYSIS	31
3.9 PROTEIN CONCENTRATION MEASUREMENT.....	32
3.10 STATISTICAL ANALYSIS.....	32
4. RESULTS	33
4.1 FLOW CYTOMETRY	33
4.2 NTA ANALYSIS.....	34
4.3 CHARACTERIZATION OF PEV BY IMMUNOCHEMICAL METHODS	39
4.3.1 PROBING FOR THE PRESENCE OF EV SURFACE MARKERS ON PEVS INDUCED BY TC/CA ²⁺ IONOPHORE ACTIVATION....	39
4.3.2 ELISA ANALYSIS	42
5. DISCUSSION	44
5.1 FLOW CYTOMETRY	44
5.2 IMMUNOCHEMICAL METHODS.....	45
5.3 DETERMINING OF BDNF LOCATION IN PEVS	47
5.4 DETERMINING THE SIZE DISTRIBUTION OF PARTICLES DERIVED FROM ACTIVATED PLATELETS.....	48

5.5	CONCLUSIONS.....	48
6.	<u>ACKNOWLEDGEMENTS.....</u>	<u>50</u>
7.	<u>REFERENCES</u>	<u>51</u>

FIGURE 1 SCHEMATIC PICTURE OF THE PLATELET DISPLAYING ALPHA AND DELTA GRANULES AS WELL AS LYSOSOMES, MITOCHONDRIA AND THE OPEN CANALICULAR SYSTEM, WHICH ARE THE SOURCE OF PROTEIN CARGO TO BE PACKED INTO PLATELETS.	11
FIGURE 2. DIFFERENT PHASES OF PLATELET ACTIVATION IN THE BLOOD CIRCULATION FROM RESTING STATE TO MICROVESICULATION, WHEN PEVs ARE SECRETED. ADAPTED FROM SILJANDER 2000.....	13
FIGURE 3 THE TWO TRANSMEMBRANE PROTEINS THAT THE NEUROTROPHINS BIND TO I.E. THE p75 AND THE TRK RECEPTORS. ADAPTED FROM BIBEL AND BARDE 2000 AND PROTEIN DATA BANK EUROPE.	14
FIGURE 4 THE BIOGENESIS, SUBCELLULAR ORIGIN AND SIZE GROUPS OF EVs AND THEIR RELEASE INTO THE EXTRACELLULAR SPACE. ADAPTED FROM YAÑEZ-MÓ AND SILJANDER ET AL. 2015.....	18
FIGURE 5 WIDELY USED METHODS FOR ISOLATING EVs. ADAPTED FROM KONOSHENKO ET AL. 2018	23
FIGURE 6 A TEST TUBE SHOWING THE RESULT OF THE BUFFY COAT METHOD.	24
FIGURE 7 FLOW CHART DISPLAYING THE PROCESS OF PLATELET ISOLATION FROM PC. THE SAMPLE WAS FIRST PELLETED BY CENTRIFUGATION. THE PELLET WAS THEN RESUSPENDED IN 1 ML OF Ca^{2+} -FREE TYRODE-HEPES BUFFER AND FINALLY THE PLATELETS WERE ISOLATED BY GEL-FILTRATION.	25
FIGURE 8 FLOWCHART DESCRIBING HOW THE PLATELET FREE PLASMA WAS PRODUCED FOR THE PROJECT.....	28
FIGURE 9 A PHOTO OF THE IODIXANOL GRADIENT USED IN THE PROJECT. A BOTTOM-UP GRADIENT WAS CHOSEN, SINCE WE WERE INTERESTED IN SEPARATING PEVs BASED ON THEIR DENSITY.	29
FIGURE 10 PLATELET ANALYSIS BY FLOW CYTOMETRY WITH THE APOGEE A50 MICRO FLOW CYTOMETER. THE PRESENTED DOT PLOTS ARE A) THE CONTROL SAMPLE STAINED WITH ANTI-CD41 B) PLATELET SAMPLE ACTIVATED BY Ca^{2+} IONOFORE STAINED WITH ANTI-CD62P C) PLATELET SAMPLE ACTIVATED BY TC CO-STIMULATION AND STAINED WITH CD62P.....	33
FIGURE 11 PARTICLE AMOUNT IN THE SAMPLES FROM THE PLATELET ACTIVATION BY TC CO-STIMULATION AND Ca^{2+} IONOFORE MEASURED BY NTA. THE CONTROL SAMPLE IS FROM THE UNACTIVATED SAMPLE. THE PARTICLE AMOUNT IN THE SAMPLES DERIVED FROM THE TC CO-STIMULATION INCREASED 1.6 TIMES IN RELATION TO THE CONTROL. THE PARTICLE AMOUNT IN THE SAMPLES DERIVED FROM THE Ca^{2+} IONOFORE STIMULATION, HOWEVER, INCREASED 14.8 TIMES IN RELATION TO THE CONTROL. THE SAMPLES WERE MEASURED AS TRIPPLICATES AND THE RESULTS ARE THE MEAN \pm SEM/SD OF THREE INDEPENDENT MEASUREMENTS. THE SD FOR THE CONTROL SAMPLE, THE TC CO-STIMULATION SAMPLE AND THE Ca^{2+} IONOFORE SAMPLE WAS 1.27, 2.9 AND 7.5 RESPECTIVELY.	34
FIGURE 12 PERCENTILE SIZE DISTRIBUTION OF THE PARTICLES AS ANALYSED BY NTA AND CORRESPONDING STATISTICAL SIGNIFICANCE. FOR ALL THREE SAMPLES THE MAJORITY OF THE PARTICLES WERE WITHIN 100-250 NM IN DIAMETER. STIMULATION BY Ca^{2+} IONOFORE PRODUCED MORE PARTICLES LESS THAN 100 NM IN DIAMETER WHEN COMPARED TO THE CONTROL AND THE TC CO-STIMULATION-DERIVED PARTICLES. THE SAMPLES WERE MEASURED AS TRIPPLICATES AND THE RESULT IS THE MEAN \pm SEM/SD OF THREE INDEPENDENT MEASUREMENTS.....	35
FIGURE 13 COMPARISON OF PARTICLE CONCENTRATION PRE- AND POST-DENSITY-GRADIENT CENTRIFUGATION. A SUBSTANTIAL SAMPLE LOSS WAS OBSERVED. WHEN COMPARING THE TOTAL AMOUNT OF PARTICLES OF THE UNCENTRIFUGED SAMPLE TO THE TOTAL PARTICLE AMOUNT IN THE SAMPLE PURIFIED BY DENSITY-GRADIENT CENTRIFUGATION THE GAIN FOR THE CONTROL SAMPLE WAS 11%. THE GAIN FOR BOTH THE PARTICLES DERIVED FROM THE TC CO-STIMULATION AND THE Ca^{2+} IONOFORE STIMULATION WAS 17%. THE SAMPLES WERE MEASURED AS TRIPPLICATES AND THE RESULT IS THE MEAN \pm SEM/SD OF THREE INDEPENDENT MEASUREMENTS.	36
FIGURE 14 DENSITY DISTRIBUTION AND CORRESPONDING SIZE OF THE PARTICLES DERIVED FROM THE TC CO-STIMULATION OF PLATELETS. THE DENSITY DISTRIBUTION OF THE PARTICLES WITHIN THE DIFFERENT SIZE GROUPS WAS ANALYSED BY NTA. PARTICLES WITH SMALLER DENSITIES DOMINATED THE GROUPS OF SMALLER DIAMETERS WHILE PARTICLES OF LARGER DENSITIES DOMINATED THE GROUPS OF BIGGER DIAMETERS.	37
FIGURE 15 DENSITY DISTRIBUTION AND CORRESPONDING SIZE OF THE PARTICLES DERIVED FROM THE STIMULATION BY Ca^{2+} IONOFORE. THE DENSITY DISTRIBUTION OF THE PARTICLES WITHIN THE DIFFERENT SIZE GROUPS WERE ANALYSED BY NTA. THE DENSITY TO DIAMETER DISTRIBUTION APPEARED FAIRLY SIMILAR TO THAT OF THE TC CO-STIMULATION. AS A RESULT OF THE Ca^{2+} IONOFORE STIMULATION, HOWEVER, THE NUMBER OF PARTICLES OF SMALLER DENSITY WAS SOMEWHAT LARGER, EFFECT OF THE UNSELECTIVE NATURE OF THE Ca^{2+} IONOFORE STIMULI.....	38
FIGURE 16 COMPARISON OF THE MEAN SIZE DISTRIBUTION OF THE ANALYSED PARTICLES. THE APPLIED STIMULUS ON THE DENSITY TO DIAMETER DISTRIBUTION DOES NOT APPEAR STATISTICALLY SIGNIFICANT. EXCEPT FOR THE PARTICLES WITH A DENSITY OF 1.112 G ML ⁻¹ , THE PARTICLES DERIVED FROM THE TC CO-STIMULUS HAD THE LARGEST MEAN DIAMETER.	39
FIGURE 17 WESTERN BLOT MEMBRANE PROBED WITH A CD9 ANTIBODY. THE ANALYSED SAMPLE WAS A TC CO-STIMULATION DERIVED PEV SAMPLE THAT WAS PURIFIED BY DENSITY-GRADIENT CENTRIFUGATION. FRACTIONS 35—22% (1.190 G ML ⁻¹ -1.112 G ML ⁻¹) WERE POSITIVE FOR CD9, WHEREAS FRACTIONS 40% (1.215 G ML ⁻¹) AND 20% (1.092 G ML ⁻¹) WERE NEGATIVE. THE STRONGEST SIGNAL WAS DETECTED IN FRACTIONS 22% AND 24% THE EXPECTED MOLECULAR WEIGHT FOR CD9 IS APPROXIMATELY 25 kDa AND IT IS INDICATED BY AN ARROW. RESULTS ARE REPRESENTATIVE OF THREE REPEATS.....	40
FIGURE 18 WESTERN BLOT MEMBRANE PROBED WITH A CD63 ANTIBODY. THE ANALYSED SAMPLE WAS A PEV SAMPLE DERIVED FROM TC CO-STIMULATION WAS THEN PURIFIED BY DENSITY-GRADIENT CENTRIFUGATION. FRACTIONS 22%-35% WERE POSITIVE FOR CD63 WHEREAS FRACTIONS 40% AND 20% WERE NEGATIVE. FRACTIONS 24% AND 22% GAVE THE STRONGEST SIGNAL. THE EXPECTED	

MOLECULAR WEIGHT FOR CD63 IS APPROXIMATELY 65 kDa IS INDICATED BY AN ARROW. DATA IS REPRESENTATIVE OF THREE REPEATS

.....	40
FIGURE 19 WESTERN BLOT PROBED FOR BDNF. THE HIGHLY POSITIVE SIGNALS IN LANE 1 AND 2 ARE PLATELET SAMPLES PRE- AND POST- ISOLATION BY SIZE EXCLUSION CHROMATOGRAPHY. THE SAMPLE IN LANE 4 IS TC CO-STIMULATION-DERIVED PEVS. THE CA ²⁺ IONOPHORE-DERIVED PEVS IN LANE 5 WERE NEGATIVE AS WERE THE UNACTIVATED PEV SAMPLES IN LANE 6. THE POSITIVE CONTROL OF MOUSE BRAIN LYSATE IN LANE 9 GAVE A VERY FAINT POSITIVE SIGNAL VISIBLE ONLY WITH OVEREXPOSURE OF THE GELS. THE EXPECTED MOLECULAR WEIGHT OF BDNF IS APPROXIMATELY 11 kDa IS INDICATED BY AN ARROW. RESULTS ARE REPRESENTATIVE OF THREE REPEATS.	41
FIGURE 20 WESTERN BLOT PROBED FOR BDNF. TC CO-STIMULATION DERIVED PEVS WERE PURIFIED BY DENSITY-GRADIENT CENTRIFUGATION. FRACTIONS 22% AND 24% WERE POSITIVE FOR BDNF WHEREAS THE OTHER FRACTIONS APPEARED TO BE BDNF NEGATIVE. RESULTS ARE REPRESENTATIVE OF THREE REPEATS. THE EXPECTED MOLECULAR WEIGHT OF BDNF IS APPROXIMATELY 11 kDa IS INDICATED BY AN ARROW	42
FIGURE 21 FIGURE DISPLAYING THE BDNF-CONCENTRATION IN THE PEV SAMPLES WHEN NORMALIZED TO PROTEIN CONCENTRATION. SAMPLES 1-5 ARE TC CO-STIMULATION-DERIVED PEVS AS A DILUTION SERIES. SAMPLES 6-9 ARE CA ²⁺ IONOPHORE CO-STIMULATION-INDUCED PEVS AS DILUTION SERIES. BOTH SAMPLE TYPES WERE DILUTED SUCH THAT THE NEXT SAMPLE IS DILUTED 1/3 IN RELATION TO THE PREVIOUS ONE. SAMPLE 10 IS THE UNACTIVATED SAMPLE, SAMPLES 11 AND 12 ARE PLATELET SAMPLES PRE- AND POST- ISOLATION BY SIZE EXCLUSION CHROMATOGRAPHY. SAMPLE 13 IS THE NEGATIVE CONTROL AND SAMPLE 14 IS THE POSITIVE CONTROL. DATA IS REPRESENTATIVE OF THREE MEASUREMENTS.	43
FIGURE 22 ANALYSIS OF BDNF CONCENTRATION/PARTICLE MEASURED BY NTA. IN THE PEV SAMPLES WE FOUND THAT THE CONTROL SAMPLE CONTAINED 0.263 PG BDNF PARTICLE ⁻¹ WHEREAS THE PARTICLES DERIVED FROM THE TC CO-STIMULATION CONTAINED 0.46 PG PARTICLE ⁻¹ . THE CA ²⁺ IONOPHORE STIMULATION DERIVED PARTICLES IN THE OTHER HAND CONTAINED 0.053 PG PARTICLE ⁻¹	44

Abbreviations

ApoB	Apolipoprotein B
ALCAM	Activated leukocyte adhesion molecule
BDNF	Brain derived neurotrophic factor
CNS	Central nervous system
ELISA	Enzyme-linked immunosorbent assay
EV	Extracellular vesicle
FITC	Fluorescein isothiocyanate
GABA	Gamma-aminobutyric acid
IONO	Ionophore
ISEV	The International Society of Extracellular vesicles
LALS	Large angle light scatter
NCAM	Neural cell adhesion molecule
NGF	Nerve growth factor
NTA	Nanoparticle tracking analysis
OCS	Open canalicular system
PAR1	Protease activated receptor 1
PC	Phosphatidylcholine
PDGF	Platelet-derived growth factor
PE	Phosphatidylethanolamine
PEV	Platelet-derived extracellular vesicle
PFP	Platelet-free plasma
POD	Peroxidase conjugated
PRP	Platelet rich plasma
PS	Phosphatidylserine
SALS	Small angle light scatter
SEC	Size exclusion chromatography
sCMOS	Scientific complementary metal-oxide-semiconductor
SM	Sphingomyelin
TC	Thrombin and collagen co-stimulus
Trk	Tropomyosin receptor kinase
VEGF	Vascular endothelial growth factor
vWF	von Willebrand factor

1. Background

1.1 Platelets

Platelets originate from megakaryocytes in the bone marrow, in blood vessels, and also in the lungs (Figure 1, Lefrançois & Looney 2019). The megakaryocyte is a polyploid hematopoietic cell. Polyploid megakaryocytes and anucleate platelets can only be found in mammals. The human body produces 1×10^{11} platelets every day and their lifespan in the blood circulation is 8-10 days. The ageing platelets are then eventually phagocytosed by macrophages in the spleen. The diameter of resting platelets is 2-4 μm and they are discoid in shape. It had been shown by means of flow cytometry, histogram and single cell analytics, that platelet populations differ from each other in both volume density as well as reactivity (Baaten et al. 2017).

Platelets are produced by pinching off from the cytoplasm of megakaryocytes (Radley and Haller 1982). Due to this process platelets do not contain any DNA. All platelets do, however, contain plenty of proteins (Burkhart et al. 2013), mRNA (Laffont et al. 2013) and microRNA (Baaten et al. 2017). This platelet cargo is then secreted following platelet activation. The environment of the developing megakaryocyte affects the properties of the platelet that pinches off from it. The platelet transcriptome of a person suffering from systemic lupus erythematosus, for instance, differs from that of a healthy control subject (Lood et al. 2010).

Megakaryocytes also contain growth promoting cytokines, such as interleukin 3 (Machlus & Italiano 2013), thrombopoietin (Machlus & Italiano 2013) and brain derived neurotrophic factor (BDNF) (Chacón-Fernández 2016). Platelets are known to perform protein synthesis (Ludány and Kellermeyer 1988) but megakaryocytes appear to be the primary source of the BDNF stored in platelets. This seems plausible, since megakaryocytes contain an easily detectable amount of BDNF (Chacón-Fernández et al. 2016). The theory is further supported by the fact that BDNF, in both megakaryocytes and platelets, is stored in alpha-granules (Maynard et al. 2007). Furthermore, BDNF has been detected in pro-platelets (Chacón-Fernández et al. 2016) making it seem probable that platelets contain BDNF already as they are pinching off from megakaryocytes.

A defining structural property of the platelet is an internal membrane system, the open canalicular system (OCS). The OCS consists of a network of channels that are connected to the platelet membrane. During platelet activation, the OCS partly fuses together with the platelet membrane, thus increasing

the membrane area to volume ratio (Escolar et al. 1989, Wachowicz et al. 2016). The OCS enables an effective internalization of surrounding molecules into the platelet. The OCS also provides membrane surface for morphological changes and it is central in the formation of extracellular vesicles (EV).

The molecules that are secreted by platelets are located in intracellular vesicles that are called granules (Figure 1). Three different kinds of granules can be distinguished –alfa- and delta-granules as well as lysosomes. The most abundant granule of the three is the alfa-granule of which 50-80 typically reside within one platelet (Frojmovic and Milton 1982). The alfa-granules are packed with molecules important for haemostasis (Figure 1), such as von Willebrand factor (vWF), CD62P and integrin $\alpha\text{IIb}\beta_3$ (Wachowicz et al. 2016) that are secreted when the OCS fuses together with the plasma membrane. A tell-tale sign of platelet activation is the appearing of granular proteins, such as CD62P, to the platelet plasma membrane. Platelet activation precedes platelet aggregation as well the secretion of EVs.

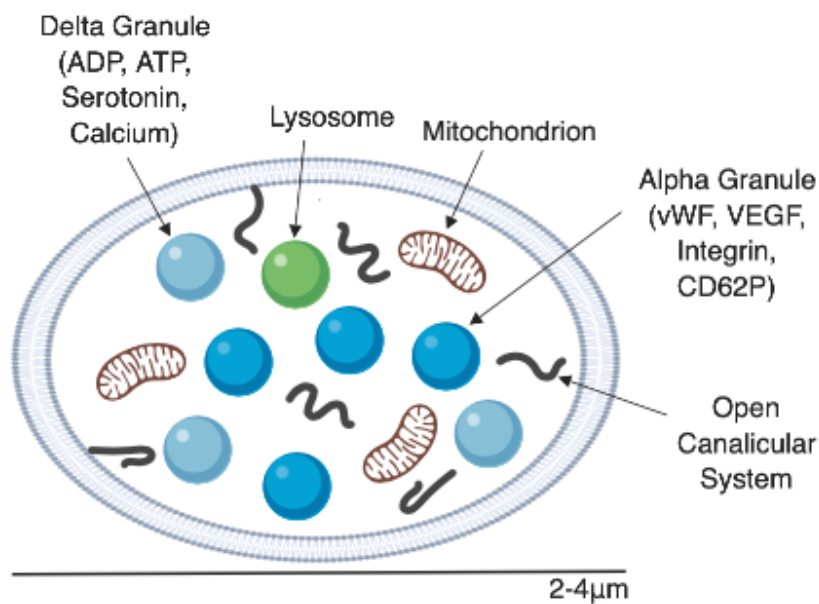


Figure 1 Schematic picture of the platelet displaying alpha and delta granules as well as lysosomes, mitochondria and the open canalicular system, which are the source of protein cargo to be packed into platelets.

The content of the alfa-granules is heterogenous and many molecules have opposing function. The content can be divided, for instance, into pro- and anti-angiogenic molecules. The vascular endothelial growth factor (VEGF) and the platelet derived growth factor (PDGF) are examples of pro-angiogenic compounds (Kaplan et al. 1979), whereas endostatin (Ma et al. 2001) and angiostatin (Jurasz et al. 2003) are examples of anti-angiogenic molecules contained within the inactive platelet. On the other

hand, the content of alfa-granules can also be classified as either pro- or anticoagulant (Blair and Flaumenhaft 2009) as well as pro- and anti-inflammatory (Golebiewska and Poole 2015) .

Besides alfa-granules, the platelets contain so called delta-granules that are rich in calcium, ADP, ATP, serotonin and histamine, as well as pyro- and polyphosphates (Meyers et al. 1982). All of these molecules, within the delta-granules, are known to support platelet aggregation, the tonus of the vasculature and the clotting of blood (Ambrosio and Di Pietro 2017). The functionality of the third class of granules in platelets, the lysosome, is not yet well understood. It is, however, clear that unlike in other cell types, the platelet lysosomes also participate in secretion (Yadav and Storrie 2016). Furthermore, it appears that the lysosomal molecules participate in thrombus formation and remodelling of the extracellular matrix (Yadav and Storrie 2016). Platelets are also known to be an important source of mitochondria in the blood (Koupenova et al. 2018). These functionally diverse molecules can all be secreted from platelets packed into EVs. These EVs, are secreted from platelets as a result of an appropriate stimulus. Depending on the stimulus, these molecules then take part in a multitude of mechanisms. Molecules such as vWF, fibrinogen and CD62P support haemostasis by participating in the coagulation cascade. Molecules such as histamine, on the other hand, participate in immunological reactions, such as the inflammatory response (Ramadan et al. 2015).

The primary function of platelets is to support the haemostatic reactions by maintaining the integrity of the blood vessels, and by participating in the activation of the coagulation cascade (Xu et al. 2016a) and profibrinolysis (Gue and Gorog 2017). Inactive platelets circulate within the blood circulation close to the walls of the blood vessels. An intact endothelial tissue provides a natural barrier against thrombosis and as such effectively hinders untimely platelet activation. The endothelium also secretes inhibitory factors, such as nitric oxide and prostacyclin, further supporting the inactive state of the platelets (Golebiewska and Poole 2015). Besides this main function, platelets also play an important part in both physiological and pathological processes, such as chronic inflammation, the immune response and in perturbances of the central nervous system, such as multiple sclerosis and Alzheimer's disease (Xu et al. 2016b).

Platelets may be activated by a discontinuity in the endothelial monolayer of the vasculature (Figure 2), and by an inflammation that irritates the endothelium (Ali et al. 2015, Sonmez and Sonmez 2017). As the underlying matrix is revealed, disrupting the monolayer, platelets are able to interact with the revealed adhesive proteins. These adhesive molecules include von Willebrand factor, collagen and soluble platelet agonists, such as thrombin of the coagulation cascade reviewed in Wachowicz et al. 2016. The interaction between platelets and the adhesive proteins of the subendothelium results in

the secretion of activating factors, such as vWF, that can further activate the platelets (Wachowicz et al. 2016). Platelets can alternatively be activated directly by the effect of agonists, such as thrombin and collagen, where the following auto-activation through secretion amplifies the response. Activated platelets secrete soluble cytokines and chemokines from their internal stockpile and in doing so attract more platelets to the site of injury to be activated (Golobiewska and Poole 2014). In this way aggregated platelets can ultimately result in a blood clot (Figure 2). Platelet activation also results in secretion of platelet derived EVs (PEV), one of the hallmarks of the activated platelet (Siljander 2011).

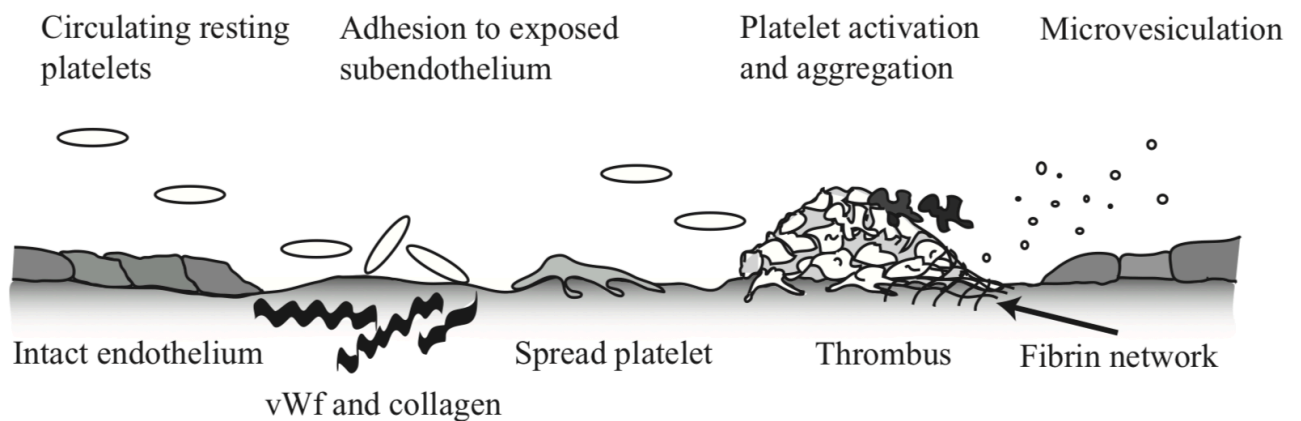


Figure 2. Different phases of platelet activation in the blood circulation from resting state to microvesiculation, when PEVs are secreted. Adapted from Siljander 2000.

Platelets and platelet rich plasma (PRP) are used to treat cancer patients, patients who have lost copious amounts of blood, surgery patients and for treating thrombocytopenia i.e. the condition where the concentration of platelets in the blood circulation is too low. PRP is also administered in order to support cell division and angiogenesis in bone healing processes, for instance (Agahaloo et al. 2002, Schliephake 2002).

1.2 Brain-derived neurotrophic factor

Brain derived neurotrophic factor (BDNF) is a member of the nerve growth factor family. Other members of this family include nerve growth factor (NGF), neurotrophin-3 and neurotrophin-4 (Castrén and Lindholm 1992). BDNF is a basic cytokine, soluble and ball like homodimer (Barde et al 1982, Dechant 2013). The hallmark of the protomer is a structure supported by disulfide bridges, typical of neurotrophins, known as cysteine knot (MacDonald et al. 1991). The cysteine knot has later been recognized in platelet-derived growth factor (PDGF), for instance, and in other secreted proteins as well (MacDonald and Hendrickson et al. 1993). The cysteine knot is also a typical structure for

cytokines and immunomodulative molecules (Lyer and Acharya 2011). A molecule containing a cysteine knot typically acts as a ligand that binds to a membrane receptor.

As hinted to by its name, BDNF is amply found in the central nervous system (CNS). There it significantly affects embryonal neural development, neuroplasticity and in adulthood also the function of memory (Bibel and Barde 2000). BDNF has also been shown to be key to cardiovascular development (Pius-Sadowska and Machaliński 2017). BDNF is synthesized within the endoplasmic reticulum as a precursor protein of 32-35 kDa known as prepro-BDNF (Kowianski et al. 2018). The prepro-BDNF is then cleaved as it is transported through the Golgi apparatus and the trans-Golgi network. ProBDNF is sorted into transport vesicles under the influence of carboxypeptidase E and the vesicles are then actively secreted from the postsynaptic dendrites (Klein et al. 1991). The terminal domain of proBDNF is finally enzymatically cleaved off by a protein convertase which produces a biologically active BDNF molecule of 14 kDa (Serra-Milàs 2016).

As predicted by the cysteine knot motif, the neurotrophins bind to two transmembrane proteins – tropomyosin receptor kinase (Trk) and the p75 receptor that is a member of the tumour necrosis factor family (Figure 3). As such the neurotrophins are able to activate cells of diverse functionalities through ligand receptor interaction. Binding of a ligand to p75 can, for instance, transmit a signal initiating cell death, whereas binding to the Trk receptor stimulates cell proliferation (Bibel and Barde 2000).

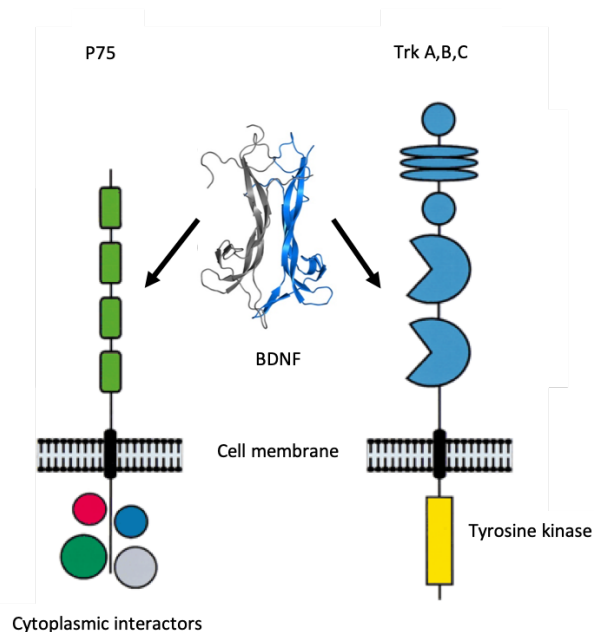


Figure 3 The two transmembrane proteins that the neurotrophins bind to i.e. the p75 and the Trk receptors. Adapted from Bibel and Barde 2000 and Protein Data Bank Europe.

The largest quantities of BDNF are found in the central nervous system (Tamura et al. 2011). BDNF is, however, also expressed in other tissues, such as the pancreas, the liver, the thyroid gland, the heart and the lungs as well (Ernfors et al. 1990, Maissonpierre et al. 1991). Monocytes, lymphocytes and eosinophils of the immune system also produce BDNF (Kerchensteiner et al. 1999). The production of BDNF in monocytes and lymphocytes is known to be of importance in protecting the nervous system (Kerchensteiner et al. 1999), whereas eosinophils produce and utilize BDNF to generate and maintain an allergic response (Raap et al. 2005). Interestingly immune cell derived BDNF has also been shown to support the survival and growth of cancer cells as well as the development of chemoresistance (Yang et al. 2006).

As noted previously, BDNF is also stored in platelets (Fujimura et al. 2002). The BDNF content within platelets is within range of the concentration in serum and higher, in fact, than the concentration in the brain (Chacón-Fernández et al. 2016). The BDNF concentration in serum is ten times higher than that of plasma (Chacón-Fernández et al. 2016). This is due to the fact that platelets secrete BDNF during coagulation (Tamura et al. 2010). Platelets store up to 90% of the BDNF in our blood and the distribution of BDNF between the platelet cytoplasm and the alfa-granule is 70:30 (Fujimura et al 2002, Tamura et al. 2011). The BDNF within the alfa-particles is secreted upon activation and the rest of the BDNF remains within the cytoplasm of the platelet (Tamura et al. 2011). When thrombin binds to the protease activated receptor 1 (PAR1) it generates a cascade that finally results in BDNF secretion (Tamura et al. 2011). VEGF and endostatin are also similarly secreted following appropriate PAR1 activation (Etulain et al. 2015). In other words, it seems likely that BDNF secreted by platelets amongst other things takes part in repairing Trk B-expressing damaged tissue (Fujimura 2002). Additionally, low BDNF concentration in serum have been observed and linked to serious depression (Shimizu et al. 2003, Serra-Millàs et al. 2011), Alzheimer's disease (Laske et al. 2007) and anorexia nervosa (Monteleone et al. 2005) as well as coronary heart disease (Amadio et al. 2019).

The calcium-induced activation of platelets and neuron bears great resemblance. Following activation both secrete neurotransmitters (Ponomarev 2018). Platelets chiefly secrete the monoamine serotonin and in smaller amounts biogenic amines, such as epinephrine, dopamine and histamine (Ponomarev 2018). Platelets also secrete the inhibiting neurotransmitter gamma-aminobutyric acid (GABA). GABA, however, is secreted in lesser amounts than the biogenic amines (Kaneez and Saeed 2009). Not unlike postsynaptic nerve cells immune cells, such as CD4-positive T cells, express ample amounts of receptors for neurotransmitters (Levite 2016, Bode and Duerschmied 2017). As such, platelets are able to directly communicate with helper T cells. Platelets, T cells and the synapses of nerve cells are also able to interact directly with antigen presenting cells via adhesion molecules and integrins (Starossom

et al. 2015, Xu et al. 2016a, Zamora et al. 2017). Some of these adhesion molecules, such as neural cell adhesion molecule (NCAM) or CD56, are expressed by both nerve cells and a subgroup of activated T cells, whereas others, such as activated leucocyte adhesion molecule (ALCAM), are expressed by nerve cells, activated T cells as well as by platelets (Ponomarev et al. 2018).

As the activation of both platelets and neurons share such striking similarities, it is safe to say that platelets are cells of importance, both immunologically and neuronally. This and the property of platelets to both store and secrete BDNF is a reason to investigate the role of platelets further in both immunological and neuronal research.

1.3 Extracellular vesicles

Most cells secrete lipid membrane enclosed vesicles that are known as EVs and they have been found in all biological fluids (Mathieu et al. 2019). The lipid membrane and cytoplasm of EVs is rich in biomolecules from the cell, from which the EV originates (van Niel et al. 2018). The amount of EVs, secreted by cells, increases by cell activation (Pasquet et al. 1996), oxidative cell stress (Mancek-Keber et al. 2015), hypoxia in the tissues (Umezū et al. 2014) and finally as a result of pathological conditions (Yañez-Mó and Siljander et al. 2015).

EVs contain DNA, RNA, lipid and protein (Gézi et al. 2019). Information about the molecular properties of EVs are comprehensively documented in open databases, such as Vesiclepedia (www.microvesicles.org/) (Kalra et al. 2012), EVpedia (www.evpedia.info) (Kim et al. 2013) and ExoCarta (www.exocarta.org) (Simpson et al. 2012). By transporting these biomolecules from one cell to another, EVs are able to affect the functions of the recipient cell. EVs participate in several essential physiological phenomena and events, such as intercellular signalling, immunity, development and differentiation (Yañez-Mó and Siljander et al. 2015). They are also involved in the development and progression of pathophysiological states, such as cancer, neurodegenerative disorders and HIV/AIDS (Gould and Raposo 2013, Mathieu et al. 2019). EVs have been isolated from most bodily fluids including plasma, cerebrospinal fluid, urine, saliva and human milk (Gézi et al. 2019, Mathieu et al. 2019).

EVs are a heterogeneous population of vesicles of different subcellular and biogenetic origin and, as such, their size, membrane structure and content are dynamic and also dependent of the cell of origin (Bebelman et al. 2018, Harada et al. 2019). Attempts have been made to classify EVs according to size, density, morphology, lipid and protein composition as well as according to subcellular origin (Akers et al. 2013, Figure 4). Up to date, however, it has not been possible to build up a scientifically

comprehensive and acceptable classification system (Théry et al. 2018). This is due to the fact that current isolation methods cannot separate pure vesicle populations (Mathieu et al. 2019), and on the other hand, since there are no specific markers for subpopulations of EVs (Théry et al. 2018, Gézsi et al. 2019).

One of the more frequently employed means of classification is categorizing EVs according to how they are formed. The first group in this classification system is exosomes. They develop from the endosomal route within multivesicular bodies and are released as the multivesicular body fuses with the cell membrane (Akers et al. 2013, Figure 4). According to this classification system the second group of EVs are the microvesicles (Akers et al. 2013, Figure 4). Microvesicles are also known as ectosomes and microparticles. They form from outwards budding and fission of the cell membrane (Al Nedawi et al. 2009, Figure 4). Apoptotic bodies make up the third group of EVs. Apoptotic bodies are freed as fragmentous structures following the blebbing of the cell membrane of the apoptotic cell (Jiang et al. 2017). Apoptotic bodies are not relevant for the scope of this thesis, as the focus is on EVs derived from activated platelets. As such, apoptotic bodies won't be further discussed. This classification system has its challenges, as it has been shown that T cell -derived exosomes, for instance, form in the same way as microvesicles (Lenassi et al. 2010). On the other hand, exosomes in general have a diameter of 30-100 nm, but they are also known to sometimes have a diameter above 100 nm. The diameter of microvesicles is 100-1000 nm, however, microvesicles are also known to sometimes have a diameter that is more than 1000 nm. In other words, size alone cannot be used to classify EVs.

As the classification system is not unambiguous and the size classes of the subgroups are partly overlapping, I will use the umbrella term EV in this thesis, without specifying which subgroup I might be referring to. This is a practice also recommended by the foremost organization for professionals working with EVs, the International Society of Extracellular vesicles (ISEV) (Théry et al. 2018).

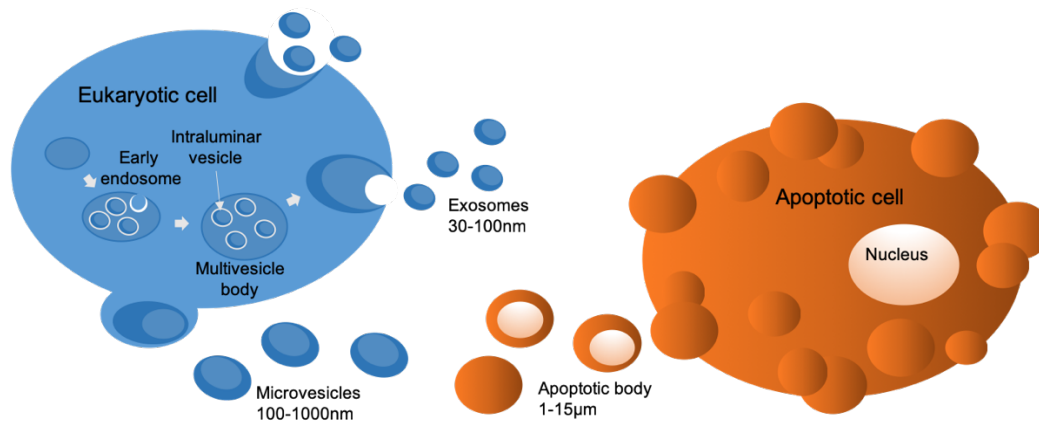


Figure 4 The biogenesis, subcellular origin and size groups of EVs and their release into the extracellular space. Adapted from Yañez-Mó and Siljander et al. 2015

EVs are secreted from the membrane of activated and apoptotic cells. Inactive cells are also, however, known to secrete small amounts of EVs (Kalra et al. 2016). The amount of EVs in the blood flow of a healthy person is at a dynamic relatively steady state (Yañez-Mó and Siljander et al. 2015). In other words, there is a balance between the secretion and clearance of EVs from the blood flow in a healthy body. EVs are known to express surface proteins, such as CD55 and CD59, that are anchored to the membrane by the glycolipid glycosylphosphatidylinositol (GPI). It is likely that EVs protect themselves from complement mediated lysis by expressing these surface proteins (Clayton et al. 2003). Thus, EVs are removed from the blood circulation either through the spleen (Davila et al. 2008), through phagocytosis by other cells (Delabranche et al. 2012), dissolved by lipases (Haggadone and Peters-Golden 2018) or by reaching the target organ, where they end up delivering their message to the cells (Jiang et al. 2017). When investigating the biodistribution of EVs from red blood cells, for instance, it has been found that 44.9% end up on the liver, 22.5% end up in the bone tissue, 9.7% end up in the epidermis and 5.8% in muscle tissue (Willekens et al. 2008).

As EVs are such a diverse population it has not been possible to determine an overall half-life for EVs in general. The clearance of EVs from different sources has been under a lot of investigation. The clearance of red cell-derived EVs has been determined as 30 minutes, for instance (Willekens et al. 2005). When investigating the clearance of PEVs, however, the results have shown great variation. The half-life for EVs expressing phosphatidylserine (PS⁺) on the cell membrane derived from platelets activated by calcium ionophore has been determined to be less than 10 minutes (Rand et al. 2006). The clearance of PEVs in the blood of patients, who have received a blood transfusion, on the other hand, has been determined to be more than three hours (Rank et al. 2011). Both of these studies were focused on PS⁺ PEVs, however, and the clearance of PS⁻ PEVs is yet to be determined.

Besides expressing surface proteins protecting EVs from complement mediated lysis, EVs also express molecules on their cell membrane that enable them to target, communicate and exchange materials with their target cell. The mechanisms by which EVs affect their target cell is comprehensively discussed in the review article by Tkach and Théry (2016). According to this review, EVs are able to initiate a messaging cascade by delivering a ligand that then interacts with an appropriate receptor on the target cell. On the other hand, EVs are also delivered into the cell by either endocytosis or phagocytosis. EVs are also able to fuse with the cell membrane and deliver their message that way. Within the cell EVs then either fuse with a lysosome or with the endocytic membranes where they unload their cargo. As EV related research is developing at a high pace, it seems likely that new mechanisms of EV mediated intercellular communication is yet to be discovered. For instance, it was shown, somewhat recently, that a nanotube like connection is necessary in the process of intercellular EV mediated mRNA trafficking (Haimovich et al. 2017).

When EV research was in its infancy it was thought that the function of these vesicles was in cellular garbage disposal. As EV research has progressed it has been shown however, that EVs do in fact have a plethora of important functions, in addition to taking care of cellular waste products. Cellular waste in this context stands for factors useless or downright harmful to the cell. For instance, as a reticulocyte matures to a mature erythrocyte EVs actively transport useless transferrin receptors out from the cell (Johnstone et al. 1989). On the other hand, the development and progression of malignant cancers is aided by the secretion of EVs with immunosuppressive properties (Wieckowski et al. 2009, Bobrie et al. 2012, Chow et al. 2014) and by actively transporting cytotoxic medications, such as doxorubicin and ciplactine, out of the tumour (Shedden et al. 2003, Safaei et al. 2005). In recent years neuron-derived EVs have also been investigated when trying to decipher CNS-related pathologies from blood biopsies (Saeedi et al. 2019).

By transporting proteins, such as enzymes and ligands, from cell to another EVs are able to affect the phenotype of the recipient cell quite rapidly. EVs have also been shown to transport cargo bearing a longer lasting and powerful effect. EVs transport mRNA and micro-RNA from one cell to another (Valadi et al. 2007). The gene expression of a cell can be turned off by an EV mediated small interfering RNA (Alvarez et al. 2011).

1.4 Platelets and extracellular vesicles

Most of the EVs in the blood circulation in a human body are platelet derived (Arraud et al. 2009). Other cells that secrete EVs into the circulation include megakaryocytes (Flaumenhaft et al. 2009), leucocytes (Pugholm et al. 2016), erythrocytes (de Vooght et al. 2013), endothelial cells (Curtis et al. 2013), smooth muscle cells (Cornelli et al. 2013) and cancer cells within the blood (Raimondo et al. 2015). Particles with procoagulant properties in plasma were first reported in 1946 (Chargaff and West 1946). These particles, PEVs, were first seen by electronmicroscopy in 1967 (Wolf 1967) and a few years later the process of platelet vesiculation was demonstrated (Warren et al. 1972). PEV and EV research really took off as late as in the early 2000s.

Platelets are enclosed by a phospholipid bilayer. This bilayer consists of PS, phosphatidylethanolamine (PE), phosphatidylcholine (PC), and sphingomyelin (SM) (Lhermusier et al. 2011). When the platelet is inactive the phospholipids of the membrane are arranged in an asymmetrical fashion. This is a central property cell physiologically speaking and it regulates the passage into and out from a cell, for instance. As such, this asymmetry is actively maintained. PC and SM typically reside on the outer membrane, whereas, PS and PE are found on the inner membrane (Lhermusier et al. 2011). The asymmetry is maintained by a set of enzymes, such as, aminophospholipid translocator, scramblase, calpain, and gelsolin (Piccin et al. 2007, Lhermusier et al. 2011). These enzymes transport aminophospholipids to the inner membrane and phospholipids to the cell surface. During PEV formation and secretion, this asymmetry is typically disrupted and negatively charged phospholipids, such as, PS and PE are revealed on the cell membrane surface (Antwi-Baffour et al. 2015). This reorganization of the phospholipids supports the coagulation cascade, for instance, since PS strongly binds to coagulation factors and coagulation factor receptors, thus supporting the progression of the formation of a thrombus (Wang et al. 2018).

The processes and molecular factors resulting in EV and PEV secretion are still somewhat unclear. It has been shown that *in vitro* PEVs are secreted as a result of both platelet activation and cell death, the stimuli being either chemical, as is the case with cytokines and endotoxins, or physical, as is the case with shear stress (Zaldivia et al. 2017). It is known, however, that EVs either pinch off from the cell membrane or fuse with the cell membrane together with multivesicular bodies. Thus, the secreted EVs carry on their surface or in their cytoplasm antigens or combinations of antigens typical of the cell of origin (Barry and Fitzgerald 1999). Consequently, since PEVs are secreted from the membrane of activated platelets, they express antigens typical for platelets and are thus recognizable as platelet

derived (Žmigrodzka 2016). Besides antigens and organelles, PEVs also transport a plethora of cytokines, enzymes, nucleic acids, and even transcription factors (Todorova et al. 2017, Zaldivia et al. 2017). There is, in fact, such a great correlation between the nucleic acids in platelets and those in PEVs that it seems likely that PEVs are a significant source of RNA in the circulation (Ray et al. 2007, Lindsey et al. 2016).

PEVs interact with the recipient cell either in a direct or in indirect way. A direct interaction indicates a situation where the EV is in itself the agent, as is the case when EVs function as a catalytic surface in the activation of coagulation factors (Kapustin and Shanahan 2016). An indirect interaction, on the other hand, indicates a situation where the recipient cell reacts to the message transmitted by the EV by changing its phenotype (Vajen et al. 2017).

PEVs develop in a manner somewhat different than EVs in general. This is because of the alfa-granules residing within the platelet. The multivesicular body, where the exosomes develop, are thought to be early forms of the alfa-granules (Heijnen et al. 1998). It is also thought that they secrete exosomes by fusing with the platelet membrane (Heijnen et al. 1999, van Nispen tot Pannerden et al. 2010). This hypothesis is supported by the fact that several molecules typical of alfa-granules have been discovered on the membrane of PEVs (Aatonen et al. 2012). One example is the protein CD63 which is a typical exosome associated protein (Gao et al. 2018). In PEVs, CD63 is also enriched in the microvesicles (van der Zee et al. 2006). On the other hand, proteins typical for microvesicles have also been found in and on platelet derived exosomes (Heijnen et al. 1999). Distinguishing the different subpopulations from each other is difficult to begin with and when working with PEVs it is that much harder. Surface proteins such as PCAM-1, CD62P (P selectin), CD63 and CD41 are typical for PEVs (Aatonen et al. 2014) making them useful when investigating PEVs. They are, however, not enough for an undisputed identification. When working with EVs it is recommended and important to validate the findings using a wide enough selection of criteria and methods (Théry et al. 2018). This holds true for PEVs as well. The characteristics and requirements for high-class EV research is an ongoing discussion in the EV community (Lötvall et al. 2014, Wittmer et al. 2017, Théry et al. 2018).

Platelets secrete small amounts of PEV when they are unstimulated (Zaldivia 2017). In order to gain enough platelets for scientific research, however, platelets need to be activated. Platelets can be activated by subjecting them to shear stress, such as vigorous shaking (Zaldivia 2017), or by treating them with agonists, such as collagen, thrombin and calcium ionophore (Siljander et al. 1996). Activation by thrombin and collagen mimics the initiation of the haemostatic / thrombotic cascade,

whereas calcium ionophore mimics a general initiation of EV secretion independent of cell type as it is based on a rise in the intracellular calcium concentration (Siljander et al. 1996).

1.5 Isolating extracellular vesicles.

Although the theme of this thesis is not the isolation methods of EVs, I want to briefly discuss the topic, since the methods of EV isolation may significantly affect the outcome of any EV-related project.

The interest the science community has towards EV related research is blooming and the hopes for health-related application of the results are finally being realised. EVs are isolated for research purposes in many different ways and these methods are often quite poorly standardised (Coumans et al. 2017). In order for research results to be comparable to other each other, reproducible and applicable, considerable effort still needs to be devoted to the development of efficient methods of isolation and analysis.

Of our bodily fluids, blood is the most researched one. At the same time, blood is the most complicated of our bodily fluids to analyse, since it on top of EVs contains cells, proteins, lipids and nucleic acids. As of yet it has not been possible to develop a method that would isolate pure EVs without any co-isolates. Thus, one needs to take into account the molecules that will co-isolate when working with EVs. Molecules that tend to co-isolate with blood derived EVs are soluble proteins, protein aggregates, lipoproteins and cellular organelles, for instance (Karimi et al. 2018).

Isolating PEVs with a sufficiently good yield free of or lipoproteins or protein-derived contaminants is a challenge (Coumans et al. 2017). From a physical point of view, the simplest way of isolating EVs is differential centrifugation and indeed a large fraction of EV isolations are preformed this way. Differential centrifugation is based on the principle that the natural sedimentation rate of particles is accelerated by the centrifugal force. The rate of sedimentation, on the other hand, is dependent on the density of the particle to be isolated in relation to the surrounding media. EVs are isolated by consecutive centrifugations with increasing centrifugal forces. EVs with higher density are isolated when applying lower centrifugal forces whereas EVs with lower density are isolated when applying higher centrifugal forces. Applying higher centrifugal forces may result in protein aggregates and EVs may also clump together (Coumans et al. 2017). The viscosity and density of plasma makes it a challenging media to work with when studying EVs. This fact combined with the lipoproteins in plasma, that have the similar density and diameter as EVs, further hampers the isolation of EVs (Théry et al. 2006, Coumans et al. 2017). A further significant challenge with isolating by means of differential

centrifugation, is the fact that it is a highly time-consuming method. By adding filters to the process, the size range of the EVs to be isolated can be regulated and in this way differential centrifugation can be made more efficient. Unfortunately, EVs are prone to taking damage when filtered if the applied force is too high (Coumans et al. 2017).

As implied by its name, density-gradient centrifugation utilises both a density-gradient and centrifugation to isolate EVs. Density-gradient is based on particles in a solution, such as EVs, with a density higher than the solution, sinking to the bottom of the test tube. Particles less dense than the solution, on the other hand, float. As a method of isolation, density-gradient is gentler than filters and the result is a contaminant free product (Aatonen et al. 2014). Sucrose or iodixanol are frequently used to create the density-gradient. Unlike sucrose iodixanol is isosmotic, inert, nontoxic and self-forming. Iodixanol is also less viscous than sucrose (Konoshenko et al. 2018) and the required centrifugation time is also shorter. Since EVs remain functional after an isolation by iodixanol, functionality assays can be performed on EVs isolated by an iodixanol gradient. Since the osmolarity remains the same, no change in volume occurs during the isolation process, and the density of the EVs remains unchanged. There are two types of gradients - the top-down gradient and the bottom-up gradient. The top-down gradient is best suited for separating EVs based on their size in diameter (Choi et al. 2011, Willms et al. 2016). The bottom-up approach, in the other hand, is best suited when isolating EVs based on the buoyant densities (Choi et al. 2011, Willms et al. 2016). The method is challenging and requires technical skilfulness, it is time-consuming and there is a risk of severe sample loss. Below is a table (Figure 5) that summarises isolation methods that are frequently employed for EV isolation. The methods are extensively discussed in the review paper by Konoshenko et al. (Konoshenko et al. 2018).

Method	Isolation principle	Pros	Cons
Ultracentrifugation	Isolation method based in density, size and shape.	Straight forward, requirements for technical skills negligent, makes large sample batches possible, high yield	Time consuming, protein complex formation, aggregation, lipoproteins of the plasma, high centrifugal velocities may damage EVs
Densitygradient ultracentrifugation	Isolation method based on density	Gentle, results in a pure product, functional vesicles	Technically challenging, laborious, time consuming, low yield
Size exclusion chromatography	Isolation method based on differences in size	Straight forward, gentle, fast, pure product	High probability for lipoprotein contamination, small sample volume
Precipitation with polyethylene glycol	Isolation method based on solubility	Straight forward, makes large sample batches possible, does not harm EVs	Contamination sensitivity, time consuming, demanding
Exoeasy	Isolation method based on affinity	Fast, makes large sample batches possible, does not harm EVs	Lipoprotein contamination, great albumin amounts

Figure 5 Widely used methods for isolating EVs. Adapted from Konoshenko et al. 2018

2. Aim of the project

The aim of the project was to investigate the BDNF content in PEVs and further to find out if the means of platelet activation has an effect on the BDNF concentration in PEV samples. We were also interested in finding the PEV subpopulations carrying BDNF and whether the BDNF concentration varied between the different subgroups. For this purpose, a density-gradient system was set up in the laboratory, during the project, to isolate PEVs.

3. Materials and methods

3.1 Isolation of platelets.

The blood used for this research was drawn from healthy volunteers who had given their informed consent according to the declaration of Helsinki. The platelet concentrates (PC) were ordered from The Finnish Red Cross Blood Service. The PC are produced by the so-called buffy coat method. The first step in this process is to centrifuge the whole blood that has been treated with an anticoagulant. By doing so the plasma (55%), the erythrocytes (45%) and the buffy coat (< 1%) are separated (Figure 6). The buffy coat includes the platelets and the leucocytes. Following the initial centrifugation, the leucocytes are carefully filtered out. The PC is produced the same day by pooling the PC of four anonymous donors. Finally, a solution, pH 7.2, consisting of sodium citrate, sodium acetate, sodium chloride, magnesium chloride and potassium chloride, is added to the PC.

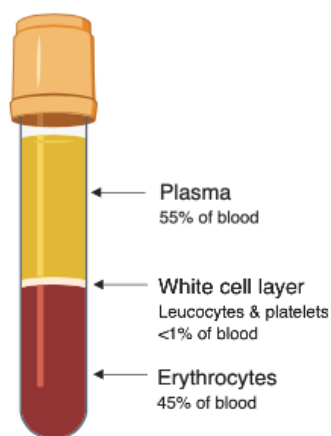


Figure 6 A test tube showing the result of the buffy coat method.

The platelets were isolated immediately upon arrival according to a protocol developed in the lab (Figure 7, Aatonen et al. 2014). 13 ml of the PC was poured into a 15 ml Falcon tube containing 100 ng ml⁻¹ prostaglandin E1 (PGE1, Sigma-Aldrich, St. Louis, the USA) and 1/6 v/v acid-citrate-dextrose buffer (ACD; 39 mM citric acid, 75 mM sodium citrate, 135 mM d-glucose, pH 4.5) which had been warmed to room temperature (RT). The sample was then centrifuged 900 × g for 15 minutes RT in a swing out rotor without applying brake in an Eppendorf 5702 R table centrifuge (Eppendorf, Hamburg, Germany). The resulting platelet pellet was resuspended thoroughly, yet carefully in a Ca²⁺ free Tyrode-Hepes buffer (137 mM NaCl, 0.3 mM NaH₂PO₄, 3.5 mM Hepes, 5.5 mM d-glucose, pH 7.35) following an addition of 100 ng ml⁻¹ PGE1, to keep the platelets from activating in advance. The platelet count was measured with a blood cell analyser (Beckman Coulter T-540, Brea, the USA) and a sample was collected. Finally, the platelets were isolated from the suspension by size exclusion chromatography in the presence of PGE1 (SEC). The CL B2 sepharose (GE Healthcare, Buckinghamshire, the UK) was balanced by washing it three times with Ca²⁺ free Tyrode-Hepes buffer. 10 ml of the sepharose was the packed into a 15 ml Telos column (Kinesis Inc., Berlin Township, the USA). 1 ml of the platelet suspension was loaded into the column and eluted with Ca²⁺ free Tyrode-Hepes buffer. 3-4 ml of the eluate was collected during the concentration peak.

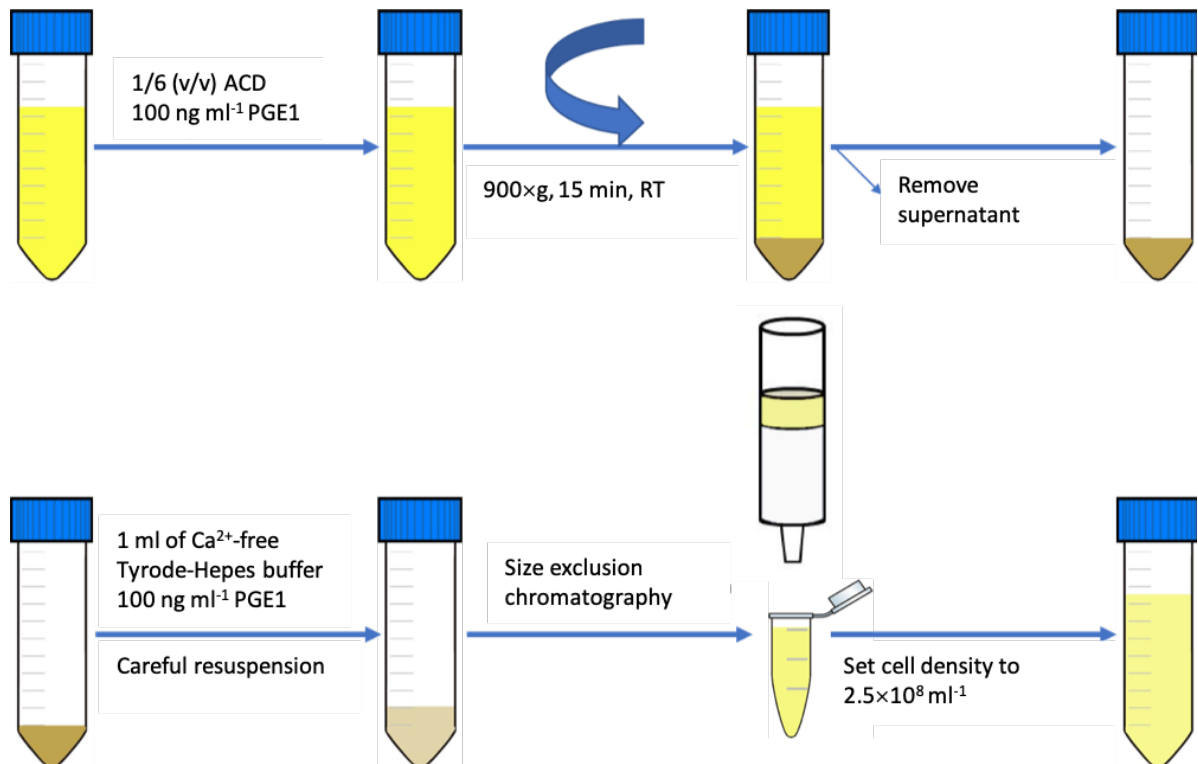


Figure 7 Flow chart displaying the process of platelet isolation from PC. The sample was first pelleted by centrifugation. The pellet was then resuspended in 1 ml of Ca²⁺-free Tyrode-Hepes buffer and finally the platelets were isolated by gel-filtration.

3.2 Activation of platelets

The platelet count of the eluate was re-measured with the blood cell analyser and the platelet concentration was adjusted to 250×10^6 platelets ml^{-1} . This platelet concentration was chosen, since it had previously been shown to be optimal when activating platelets for EV secretion (Aatonen et al. 2014).

Platelets secrete PEVs as a response to strong agonists or following a peak in the intracellular calcium concentration (Siljander et al. 1996). Based on previous observations (Aatonen et al. 2014) it was hypothesized that BDNF would be found in the so call exosome fraction following a co-stimulation by thrombin and collagen (TC co-stimulation). A TC co-stimulation was performed by pipetting 1 U ml^{-1} of thrombin and $5 \mu\text{g ml}^{-1}$ of collagen on the wall of an Eppendorf tube prior to adding the platelet suspension. The rise in the intracellular calcium concentration was mimicked by pipetting $10 \mu\text{M}$ of Ca^{2+} ionophore to the wall of an Eppendorf tube prior to the addition of the platelet suspension. In addition to TC and Ca^{2+} ionophore 1 mM MgCl_2 , 2 mM CaCl_2 and 3 mM KCl_2 were added to all of the tubes. These ions are added in order to support the activation cascade. The control sample was a platelet suspension sample that was left unactivated, yet otherwise treated exactly as the activated samples. The samples were incubated for 30 minutes at 37°C without mixing. Finally, $50 \mu\text{l}$ of the activated platelet sample was extracted for staining prior to analysis by flow cytometry. The rest of the sample was used for isolation PEVs.

Following activation, the activated platelet samples for flow cytometry were stained for 15 minutes at 37°C without mixing. As instructed by the manufacturer, $50 \mu\text{l}$ of the platelet sample was stained with $20 \mu\text{l}$ of the appropriate fluorescent antibody. Following the incubation, $450 \mu\text{l}$ of Tyrode-Hepes buffer was added to the tubes in order to stop the reaction by dilution. For this part of the project, we used the fluorescent monoclonal antibody mouse anti-human CD62P (clone AK-4, BD Biosciences, USA) conjugated with R-phycoerythrin (PE) as well as the mouse IgG1 κ isotype control (clone MOPC-21, BD Biosciences) conjugated with PE. The other antibody that we used was the monoclonal antibody mouse anti-human CD41a (clone HIP8, BD Biosciences, Franklin Lakes, The USA) conjugated with fluorescein isothiocyanate (FITC) and the mouse IgG1 κ isotype control (clone MOPC-21, BD Biosciences, Franklin Lakes, The USA) conjugated with FITC.

3.3 Isolation of PEVs

Following the activation of platelets, the platelets and other cell fragments were removed from the platelet suspension by three consecutive centrifugations. The first centrifugation was 5000×g, 5 minutes, RT (Mikro 200R, Andreas Hettich GmbH & Co. Tuttlingen, Germany). In order to make the pellet firmer the suspension was immediately centrifuged again at 11 000 ×g, 1 minute, RT (CM-50 centrifuge, Elmi Ltd. Riga, Latvia). The supernatant was transferred to a new tube and centrifuged at 2 500×g, 15 minutes, RT (Mikro 200R). To make sure that the supernatant was free from platelet contamination, a sample was analysed with the blood cell analyser. The final supernatant was then transferred into a new tube and stored at -80 °C. Before freezing the supernatant, however, a sample of 100 µl was taken and stored at -20 °C. This sample was used for the ELISA analysis.

3.4 Platelet and EV flow cytometry

The platelet activation was analysed by a second-generation flow cytometer, ApoGee A50 Microflow, capable of EV detection (Apogee flow systems, Hempstead, the UK). Platelet optimised settings were employed for the analysis. The device contains two lasers. The 405 nm laser measures scatter and the 488 nm laser measures fluorescence. The platelet gates were set for small angle light scatter (SALS) and large angel light scatter (LALS) detectors. The voltage for SALS was set to 280 V and for LALS it was set for 488 V. We also measured with detectors for 488-green and 488-orange. The voltage for these was set for 500 V and 788 V correspondingly. The gain value was set for 1 and the background was kept below 0.5. The threshold for SALS was set for 14 and 33 for LALS. Silica beads, with a refractive index similar to that of biological particles and a size between 110 nm and 1 300 nm, were used to the asses the performance of the machinery. For each measurement, 150 µl of the previously activated samples was analysed. Each measurement lasted for 120 seconds, the flow speed was 4.51 µl min⁻¹ and the machinery was meticulously rinsed following each measurement.

3.5 Density-gradient

A 60% (w/v) iodixanol (OptiPrep™, Sigma Aldrich, Missouri, the USA) in sterile water. The density of 60% (w/v) iodixanol is 1.32 g ml⁻¹. According to the manufacturer this density-gradient is well suited for isolating cells, cell organelles, viruses and proteins. The method was optimized using platelet free plasma (PFP) as we did not have instructions based on previous experiments to go by. The PFP was produced from the same PRP as the EV-rich supernatant was isolated (Figure 8). The PFP was then

purified by density-gradient centrifugation. Western blot was used to confirm that we had successfully isolated particles expressing EV typical marks CD63 and CD9 (Figure 20 and 21) and that the method was suited for PEV isolation.

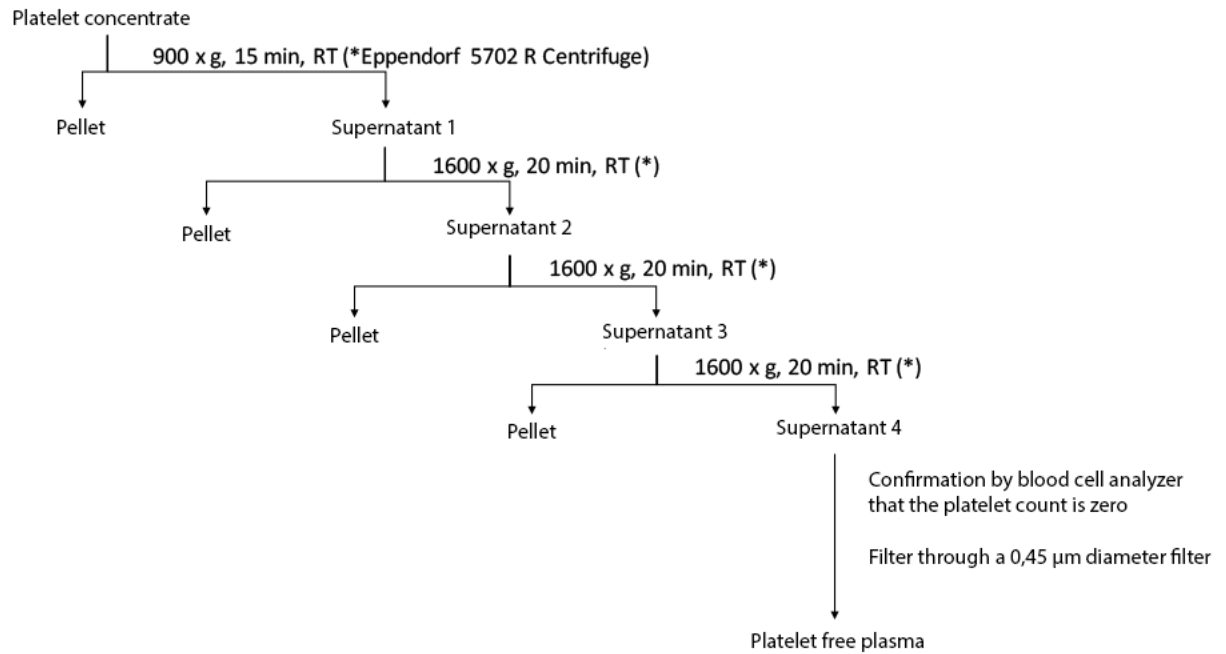


Figure 8 Flowchart describing how the platelet free plasma was produced for the project

3.5.1 Applying the density-gradient method

A discontinuous 40%-22% iodixanol gradient was pipetted into 13 ml centrifugation tubes (Ultra-Clear™, Beckman Coulter, Pasadena, USA) (Figure 9). Each fraction in the gradient was one ml, except for the 40% fraction at the bottom of the tube which was three ml. The density of the fractions was confirmed by densitometry. Thus, the density of the fraction on the bottom of the tube was 40% and the confirmed density was 1.215 g ml⁻¹. The OptiPrep™ concentration of following fractions was 35% -22% and the corresponding densities were between 1.190 g ml⁻¹ and 1.112 g ml⁻¹. Hepes-buffer (10 mM Hepes -140 mM NaCl, pH 7.4) was used as diluting agent for the OptiPrep™. As we were interested in isolating EVs based on their density, a bottom-up gradient was pipetted. The bottom fraction was created by pipetting one ml of the sample to two ml of undiluted OptiPrep™. The following one ml fractions were then pipetted on top of the bottom one. The tubes were ultracentrifuged at 100 000×g_{avg} for 16 hours at +4 °C. (SW40Ti rotor, Beckmann Coulter, Pasadena, USA). The fractions were collected, top to bottom, the following day and diluted 1:20 in Hepes buffer. The fractions were then ultracentrifuged at 100 000×g for two hours at +4 °C (Ti 50.2 rotor, Beckmann Coulter, Pasadena, USA). Following this final centrifugation, the pellets were resuspended in 200 µl Hepes buffer and stored at -80°C until analysis.

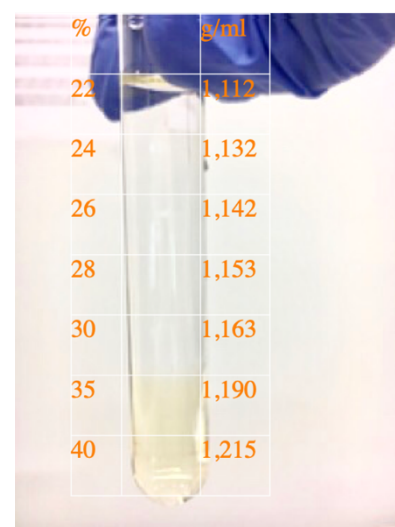


Figure 9 A photo of the iodixanol gradient used in the project. A bottom-up gradient was chosen, since we were interested in separating PEVs based on their density.

3.6 Determining the size distribution and concentration of the EV populations

Small particles in liquid, including EVs, can be directly observed and analysed in real-time with nanoparticle tracking analysis (NTA). The investigated particles are visualized by light scatter using light microscopy. A recording is made of the measurement and the NTA software tracks the Brownian movement of each individual particle and calculates the sample specific size distribution and concentration based on this.

For the size and concentration determination of the PEV we used an NTA device (LM14C, Nanosight, Malvern Instrument, Salisbury, the UK) equipped with a scientific complementary metal-oxide-semiconductor (sCMOS) camera and a 405 nm blue diode laser (Hamamatsu Photonics K.K.,

Hamamatsu City, Japan). When necessary the device was calibrated with 0.2 mm Fluoresbrite Multifluorescent Microspheres (Polyscience, Warrington; the USA). The results were analysed with the NTA 3.0 operating system. The analysis settings were expert, back-ground-extraction, auto blur, and autominimum track length on. The smallest expected particle was set for 50 nm as the cut-off value for EV measurements by NTA is 70 nm. Particle detections below 70 nm are not reliable. The samples were injected manually with a one ml Terumo syringe (Terumo Corporation, Shibuya, Tokyo, Japan) such that the sample chamber became full. The measurements were performed as 60 second triplicates per sample at a measuring temperature of 25 °C. The samples were diluted in Hepes buffer such that the sample concentration was approximately 40-100 particles frame⁻¹. This particle amount corresponds to 10⁸-10⁹ particles ml⁻¹.

3.7 SDS-Page and Western blot

Before the ELISA analysis, the PEV samples were probed for BDNF and EV markers by SDS-Page and Western blot. The positive and negative BDNF controls were a kind gift from Eero Castrén's group (University of Helsinki). The positive control was a brain lysate of a wild type mouse and the negative control was the brain lysate of a BDNF- knockout mouse i.e. the BDNF coding gene had been silenced in the knockout mouse. The PC sample and the SEC-purified platelet samples were also considered as positive controls. The protein concentration of the mouse brain lysates used as controls was determined by a commercial kit (DC Protein Assay, BioRad, Hercules, the USA) and measured with a Multiscan EX spectrometer (MTX LabSystems Inc., Bradenton, the USA). The protein concentration of the PEVs was not determined at this point, since the samples had not been purified and therefore, it was impossible to know what part of the protein concentration was constituted by PEVs and what was something else. As such the protein concentration would not have been useful information for determining the amount of sample needed for the SDS-Page analysis. Since BDNF had not previously been probed from in PEV samples we decided to add as much sample on to the gel as possible. The proteins in the samples were separated on a self-cast gel that depending on the sample type was 10%-15%. Consequently 50 µl of the PEV rich supernatant per well and 50 µg of the control samples per well was pipetted into the wells. When analysing the samples purified by density-gradient centrifugation 50 µl was also the amount pipetted per well. The samples preceding, and following SEC were presumed to be a lot more protein rich and thus only 20 µl well⁻¹ was loaded onto the gel. The samples were run at 80 V-120 V until the sample front was close to the lower edge of the running gel.

Following the gel electrophoresis, the proteins were transferred onto a methanol activated PVDF membrane (EMD Millipore Corporation, Burlington, the USA) by electrophoresis. The so-called wet blot protocol was used in this project and the proteins were transferred for one hour at a constant voltage of 100 V. The membranes were then incubated for at least two hours in 5% milk-TBST-buffer (50 mM Tris, 150 mM NaCl, 0.01% Tween). Following the blocking the PVDF membranes were incubated with the primary antibody for a minimum of two hours. The membranes were then washed three times for 15 minutes in TBS-T buffer. In this project the membranes were probed with anti-BDNF (1:1500 dilution) (Clone 3C11, Icosagen, Tartu, Estonia), anti-CD-41(1:2000 dilution) (Clone SZ22, Beckman Coulter, Brea, the USA) and anti-CD9 (1:500 dilution) (Clone M-L13, Beckton Dickinson, NJ, the USA) and anti-CD63 (1:500 dilution) (Clone H5C6, Beckton Dickinson, Franklin Lakes, the USA). The membranes were then washed three times with TBS-T for 15 minutes. Following the washes, the membranes were incubated for 45 minutes with the secondary antibody (1:2000 dilution), HRP-conjugated anti-mouse IG (GE Healthcare, Chicago, the USA). Finally, the membranes were again washed three times for 15 minutes and they were then incubated for 5 minutes in Clarity Western ECL substrate (Bio-Rad Laboratories, Hercules, the USA). The membranes were developed on Amersham Hyperfilm ECM film (GE Healthcare Lifesciences, Little Chalfont, the UK) or detected by luminescence by a Las3000 LITE luminescent image analyser (Fuji, Valhalla, the USA).

3.8 ELISA analysis

For the determining of the BDNF concentration by enzyme-linked immunosorbent assay (ELISA) instructions by Roche from 2006 were employed. The method was routinely used in the laboratory. Unless otherwise stated, all of the reagents in this part were by Roche (Hoffman-La Roche, Basel, Switzerland). We used the so-called indirect ELISA method, since it is very well suited for determining the total concentration of an antibody in a sample. This is a two-step ELISA consisting of two binding processes. The primary anti-body is first incubated with the antigen and this is followed by an incubation with an enzyme conjugated secondary antibody.

In the first part of this analysis 200 µl of the primary anti-body, anti-BDNF #1, diluted 1:4000 in carbonate buffer, pH 9.7 (50 mM NaHCO₃, 50 mM Na₂CO₃) was pipetted onto a 96-well plate. The plate was incubated overnight on a shaker at +4 °C. The following day the carbonate buffer was discarded. Now 300 µl of Hanks buffer pH 7.4 (125 mM NaCl, 5mM KCl, 1,2 mM NaH₂PO₄, 1 mM CaCl₂, 1,2 mM MgCl₂, 1 µM ZnCl₂, 10 mM glucose, 25 mM Hepes, 0,25% BSA, pH adjusted with NaOH) to which 2% BSA and 0.1% v/v had been added, was pipetted into the wells. The plate was again

incubated over night at +4 °C on a shaker. The next day the samples were pipetted onto the plate. The samples had been diluted in Hanks buffer in such a way that the same amount of sample was used as in SDS-Page and the final volume was 170 µl. 30 µl of peroxidase conjugated (POD) anti-body #9 (anti-mouse) was pipetted onto the plate as well. This secondary antibody had been diluted 1:1900 in Hanks buffer with added 6.66% BSA and 0.66% v/v Triton x-100 (Sigma Aldrich, St Louis, the USA). Thus, the final 200 µl sample contained 1% BSA, 0.1% v/v Triton x-100 and 16 mU BDNF-POD. This was followed by a third overnight incubation at +4 °C on a shaker. The following day the buffer was discarded, and the 96-well plate was washed three times with 300 µl well⁻¹ of PBS-T buffer (137 mM NaCl, 2.7 M KCl, 10 M Na₂HPO₄, 1.8 M KH₂PO₄, 0.1% Tween-20). The protein concentration in the standards were 0, 4, 8, 16, 24, 32, 48, 64, 96 and 138 pg ml⁻¹. For the detection 200 µl of POD substrate was added into each well. The samples were incubated in the dark for 20 minutes at room temperature. The reaction was then stopped by adding 50 µl of 1 M H₂SO₄ into each well. By adding the sulphuric acid, the pH in the sample changes so drastically it renders the enzyme inactive and hence the reaction is forced to a stop. The samples are then analysed by the ELISA software (Varioscan® Flash, Thermo Fischer, Waltham, the USA), and in Excel.

3.9 Protein concentration measurement

The protein concentration of both the PEV samples and for the BDNF standards was determined by Bio-Rad's DC protein assay kit (Bio-Rad, Ca, the USA). The standards for the measurement (2.0 mg ml⁻¹, 1.5 mg ml⁻¹, 1.0 mg ml⁻¹, 0.5 mg ml⁻¹, 0.2 mg ml⁻¹) were produced by diluting an albumin standard (Bio-Rad) in the same buffer as the one the samples were in. According to the manufacturer's instructions 5 µl of both standard and sample was pipetted onto a dry and clean microtiter plate (Greiner Bio One, Austria). Samples and standards were pipetted as triplicates. According to the instructions 25 µl of reagent A and 200 µl of reagent B was pipetted into six wells. The samples were then gently mixed to avoid creating bubbles. Following a 15-minute incubation at room temperature the absorbance was measured at wavelength 560 nm by a spectrophotometer (LabSystems Multiscan EX, Thermo Fischer, MA, the USA). The results were then analysed by Excel.

3.10 Statistical analysis

The results were analysed with the GraphPad Prism software (GraphPad Software Inc., version 8.3.0). The statistical significance between two groups were analysed by a paired student's *t*-test. A *p*-value of ≤ 0.05 was considered statistically significant.

4. Results

4.1 Flow cytometry

In order to assess the success of the platelet activation we analysed the samples by flow cytometry. We had previously stained the samples of activated platelets and these samples were now analysed with a second-generation Apogee A50 Micro Flow Cytometer.

Sample A (Figure 10) is the unstimulated control sample stained with anti-CD41. The analysis for CD41 was done in order to ensure that the particles were indeed platelet derived and that they had remained inactive during the isolation process. Sample B (Figure) is the sample derived from Ca^{2+} ionophore stimulated platelets (Figure 10). The ApoGee data shows that in the stimulated sample 91.51% of the particles were positive for CD62P i.e. activated. Sample C (Figure 10) is the sample derived from TC co-stimulated platelets. When analysing these samples, the data showed that 90.1% of the particles in the stimulated samples were CD62P positive i.e. activated.

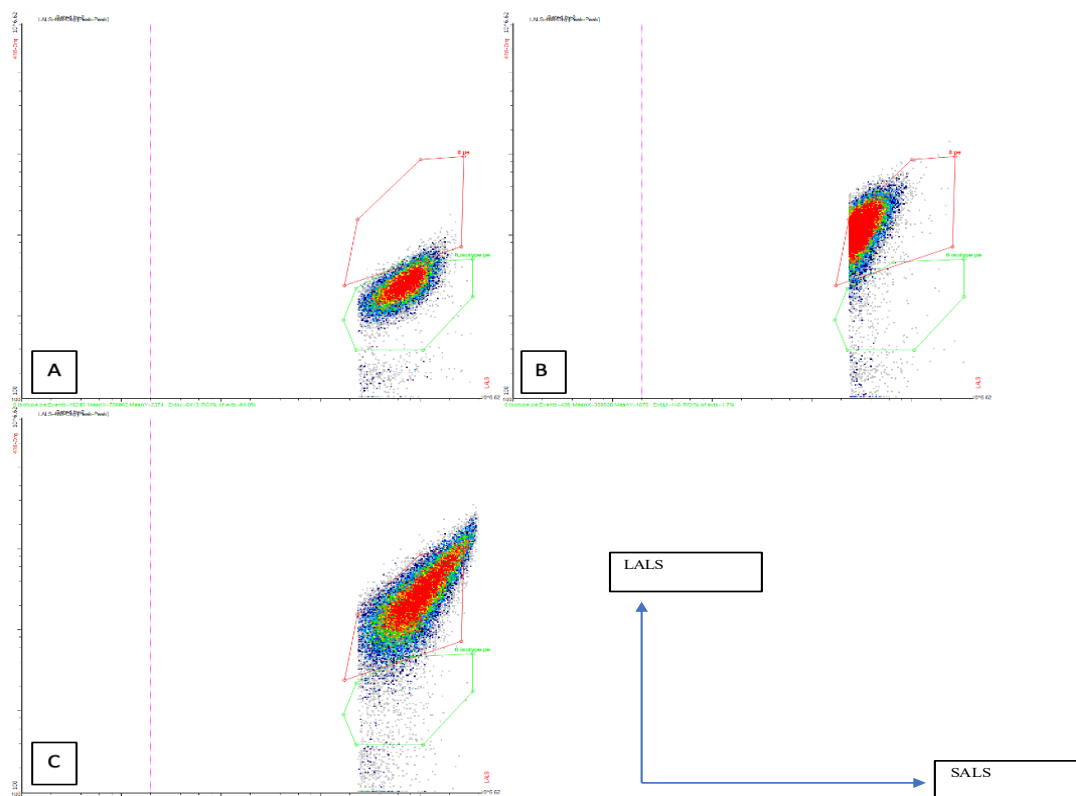


Figure 10 Platelet analysis by flow cytometry with the Apogee A50 Micro Flow Cytometer. The presented dot plots are A) the control sample stained with anti-CD41 B) platelet sample activated by Ca^{2+} ionophore stained with anti-CD62P C) platelet sample activated by TC co-stimulation and stained with CD62P

4.2 NTA analysis

Next, we wanted to compare the yields of PEVs after the different stimulations. The size distribution and concentration of the particles produced by TC co-stimulation and Ca^{2+} ionofore stimulation was analysed by NTA after total removal of platelet remnants. The NTA does not discriminate between particles, it detects all of them regardless if they are EVs, lipoproteins or protein aggregates. As such, we refer to particles, when discussing NTA results and not EVs, although lipoproteins and aggregates are less of a problem when we use isolated platelets rather than plasma. The samples were diluted such that 40-100 particles/ frame were obtained. This particle concentration approximately corresponds to 5×10^8 particles ml^{-1} which is considered the optimal concentration of particles for analysis.

Based on the NTA analysis (figure 11) the particle amount in the sample derived from the TC co-stimulation increased 1.6 in relation to the control ($p = 0.037$). The control sample contained particles from the inactivated sample. The particle amount in the Ca^{2+} co-stimulation derived particles increased significantly more – 14.8 times when compared to the control sample ($p = 0.032$). The results are a mean of three independent measurements and each measurement was carried out as triplicates.

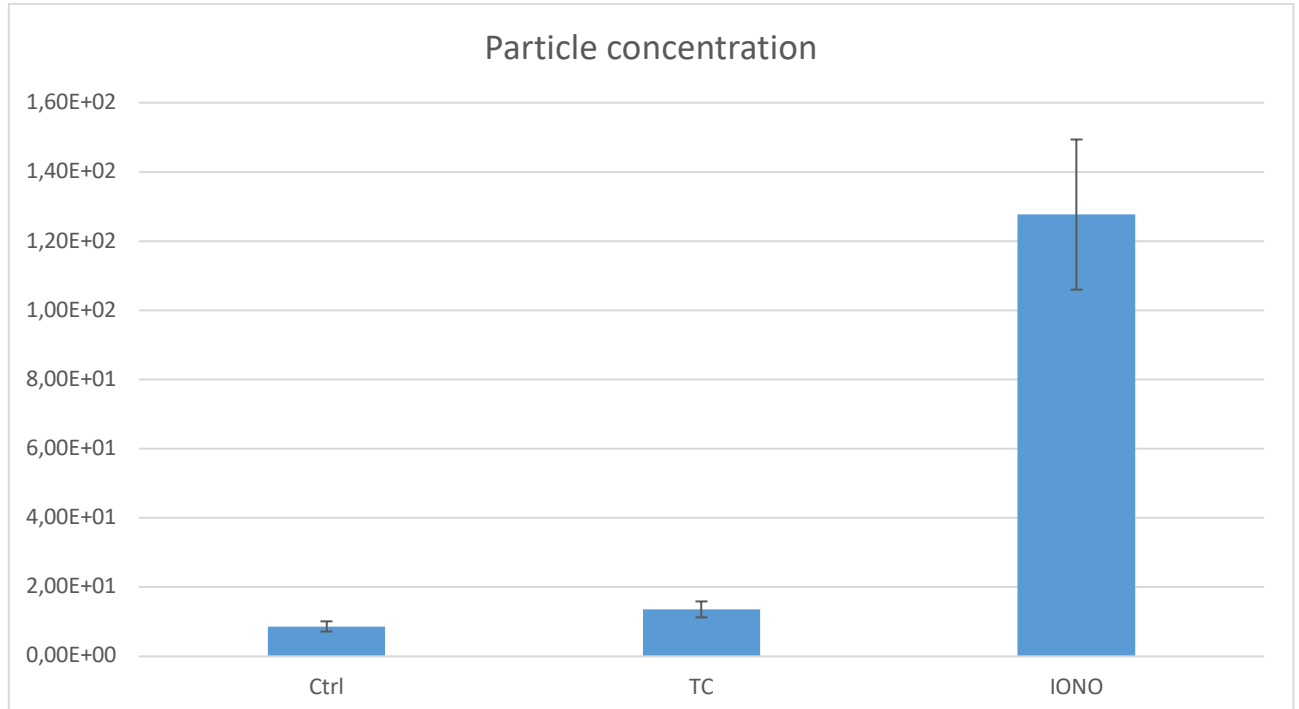


Figure 11 Particle amount in the samples from the platelet activation by TC co-stimulation and Ca^{2+} ionofore measured by NTA. The control sample is from the unactivated sample. The particle amount in the samples derived from the TC co-stimulation increased 1.6 times in relation to the control. The particle amount in the samples derived from the Ca^{2+} ionofore stimulation, however, increased 14.8 times in relation to the control. The samples were measured as triplicates and the results are the mean \pm SEM/SD of three independent

measurements. The SD for the control sample, the TC co-stimulation sample and the Ca²⁺ionofore sample was 1.27, 2.9 and 7.5 respectively.

The precentral size distribution of the particles in the samples was also analysed by NTA (Figure 12). Three independent measurements were performed, and each measurement was repeated three times. The majority i.e. 61.5% of the particles in all three sample types were 100-250 nm in diameter. Stimulation by Ca²⁺ionofore produced twice as many particles with a diameter less than 100 nm when compared to the control sample ($p = 0.027$) and three times as many as when compared to TC co-stimulation ($p = 0.003$). This corresponded well to previous results from the laboratory (Aatonen et al. 2014). Of the particles derived from the Ca²⁺ionofore stimulation, approximately 14% had a diameter between 250 nm and 500 nm. The particle amount in this size class was larger in both the control sample and the particles derived from the TC co-stimulation, 24.42% and 29.32% correspondingly. In all three sample types a very small amount of the particles represented a size class larger than this.

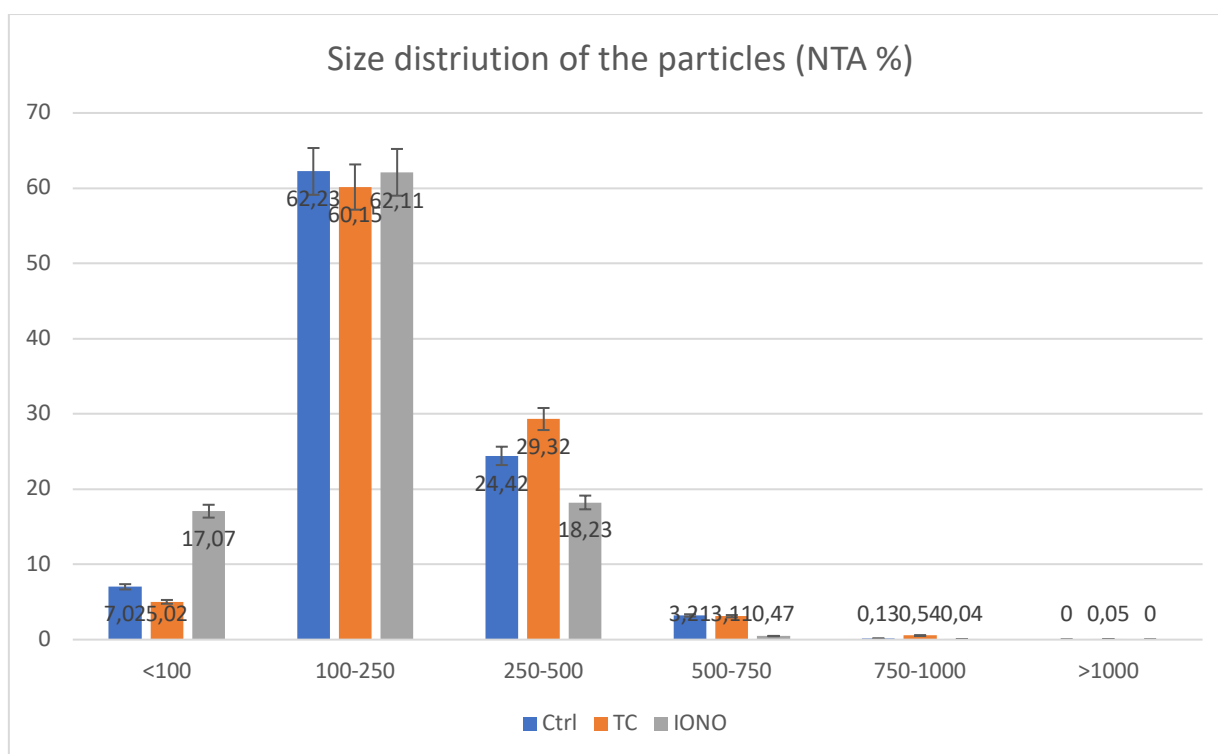


Figure 12 Percentile size distribution of the particles as analysed by NTA and corresponding statistical significance. For all three samples the majority of the particles were within 100-250 nm in diameter. Stimulation by Ca²⁺ionofore produced more particles less than 100 nm in diameter when compared to the control and the TC co-stimulation-derived particles. The samples were measured as triplicates and the result is the mean \pm SEM/SD of three independent measurements

The yield of the samples purified by density-gradient centrifugation was analysed by NTA (Figure 13). When considering the total particle amount, a large loss of sample was observed. When comparing the total amount of particles of the uncentrifuged sample to the total particle amount in the sample purified by density-gradient centrifugation the yield for the control sample was 11% (SD = 2.1). The yield for both the particles derived from the TC co-stimulation and the Ca^{2+} ionophore stimulation was 17% (SD = 2.7).

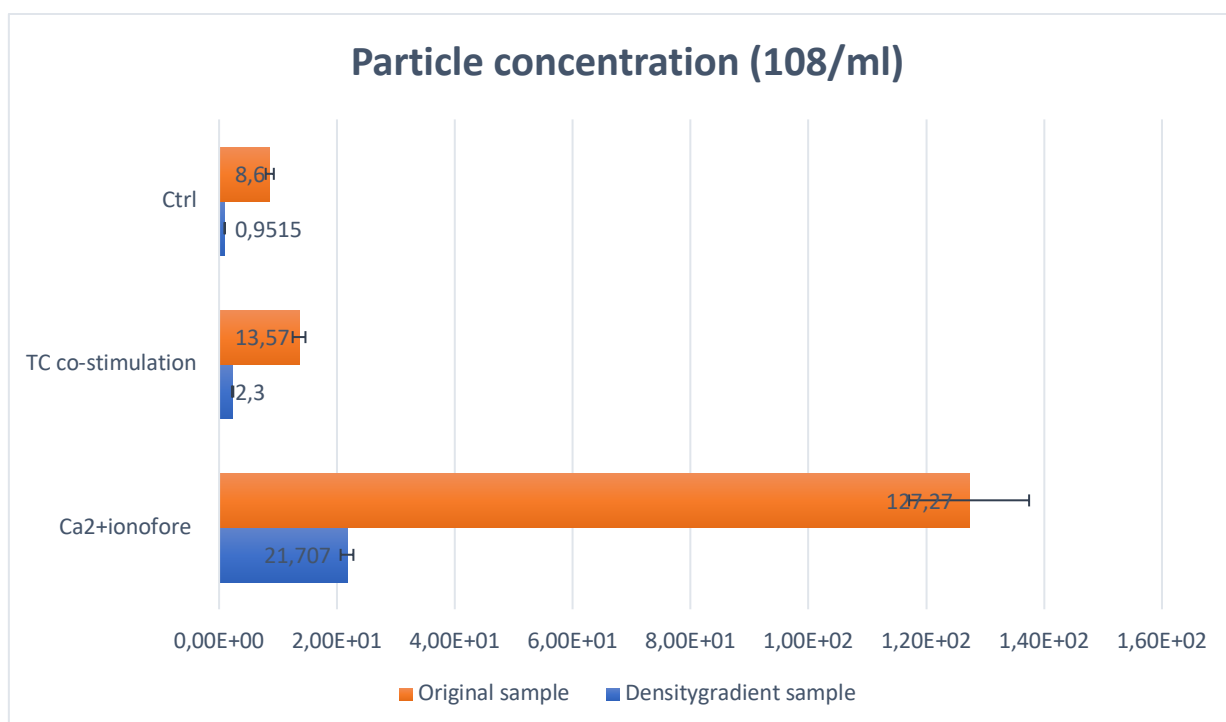


Figure 13 Comparison of particle concentration pre- and post-density-gradient centrifugation. A substantial sample loss was observed. When comparing the total amount of particles of the uncentrifuged sample to the total particle amount in the sample purified by density-gradient centrifugation the gain for the control sample was 11%. The gain for both the particles derived from the TC co-stimulation and the Ca^{2+} ionophore stimulation was 17%. The samples were measured as triplicates and the result is the mean \pm SEM/SD of three independent measurements.

The size distribution of the particles derived from the TC co-stimulation was also analysed by NTA as percentile (Figure 14). All collected fractions were analysed and the particle richest fraction was expected to be within the density group 1.112 g ml^{-1} - 1.142 g ml^{-1} (Konoshenko et al. 2018). The particles with a density of 1.112 g ml^{-1} had a mean size of 140 nm in diameter. These particles dominated the groups <100 nm and 100-250 nm. Particles in the density group 1.132 g ml^{-1} had a mean size of 256 nm in diameter and they were plentiful in the groups 100-250 nm and 250-500 nm. Particles with a density of 1.142 g ml^{-1} had a mean size of 432 nm in diameter. Particles with a density of 1.153

g ml⁻¹ had a mean size of 443.5 nm in diameter. Particles with the density 1.163 g ml⁻¹ had mean size of 478.5 nm in diameter. Particles with the density 1.19 g ml⁻¹ had mean size of 580 nm. Finally, particles with a density of 1.215 had a mean size of 609 nm in diameter. This data fits previous data well (Aatonen et al. 2014).

The particles of smaller densities i.e. 1.112-1.142 g ml⁻¹ were the most abundant ones in the particles with a mean size between 250 and 500 nm in diameter. They were less frequent in the group with a particle size of 500-750 nm in diameter, and they were non-existent in the group with particles with a diameter between 750 and 1000 nm.

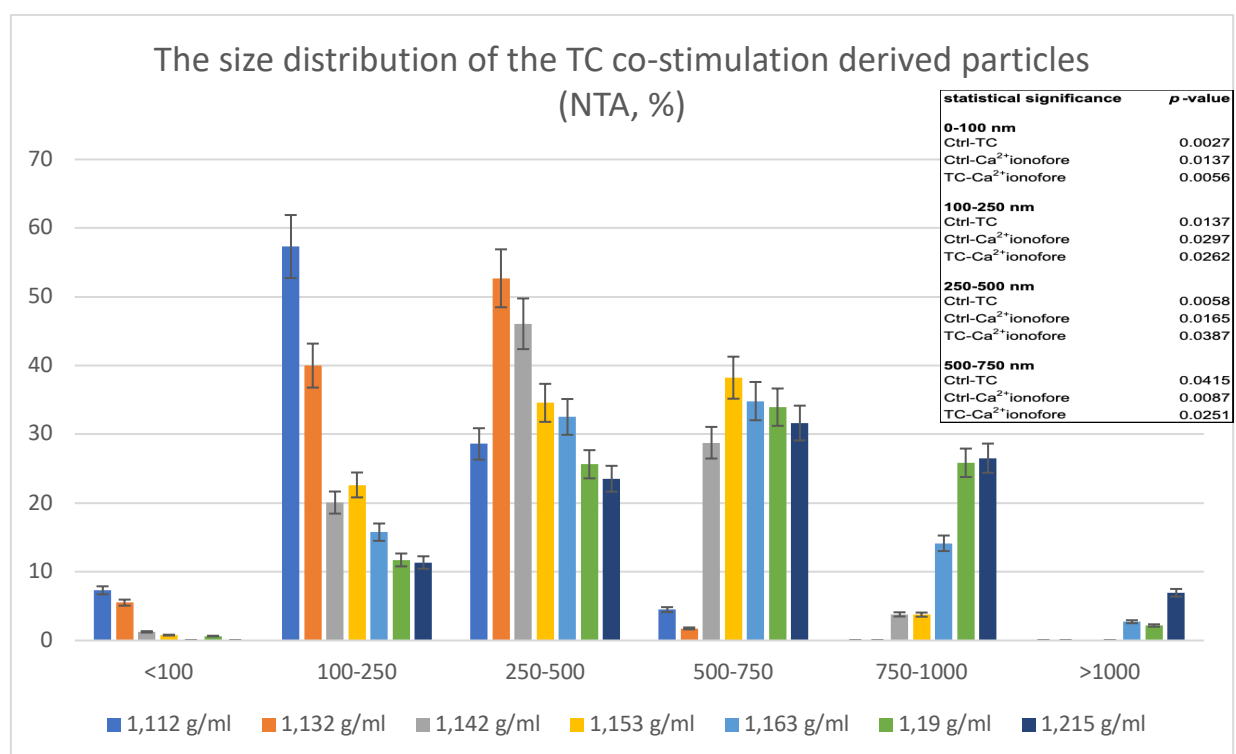


Figure 14 Density distribution and corresponding size of the particles derived from the TC co-stimulation of platelets. The density distribution of the particles within the different size groups was analysed by NTA. Particles with smaller densities dominated the groups of smaller diameters while particles of larger densities dominated the groups of bigger diameters.

The particles from the Ca²⁺ionofores stimulation were also analysed by NTA (Figure 15). The results were quite similar as for the particles from the TC co-stimulated samples. However, it seems that the number of particles with a diameter less than 250 nm were somewhat more frequent in particles from the Ca²⁺ionofores stimulation. A variation was also discovered regarding the mean size distribution of

the particles. The mean diameter of particles with a density of 1.112 g ml⁻¹ was 163.3 nm. The mean diameter of particles with a density of 1.132 g ml⁻¹ was 242.5 nm. For particles with a density of 1.142 g ml⁻¹ had a mean size of 345 nm in diameter. For particles with a density of 1.153 g ml⁻¹ had a mean size of 440 nm in diameter. Particles with a density of 1.163 g ml⁻¹ had a mean size of 440 nm in diameter. Particles with a density of 1.163 g ml⁻¹ had mean diameter of 454 nm. The mean diameter of particles with a density of 1.19 was 539.8 nm. Finally, the particles with a density of 1.215 g ml⁻¹ had a mean diameter of 541 nm. Statistically, however, this variation was not significant.

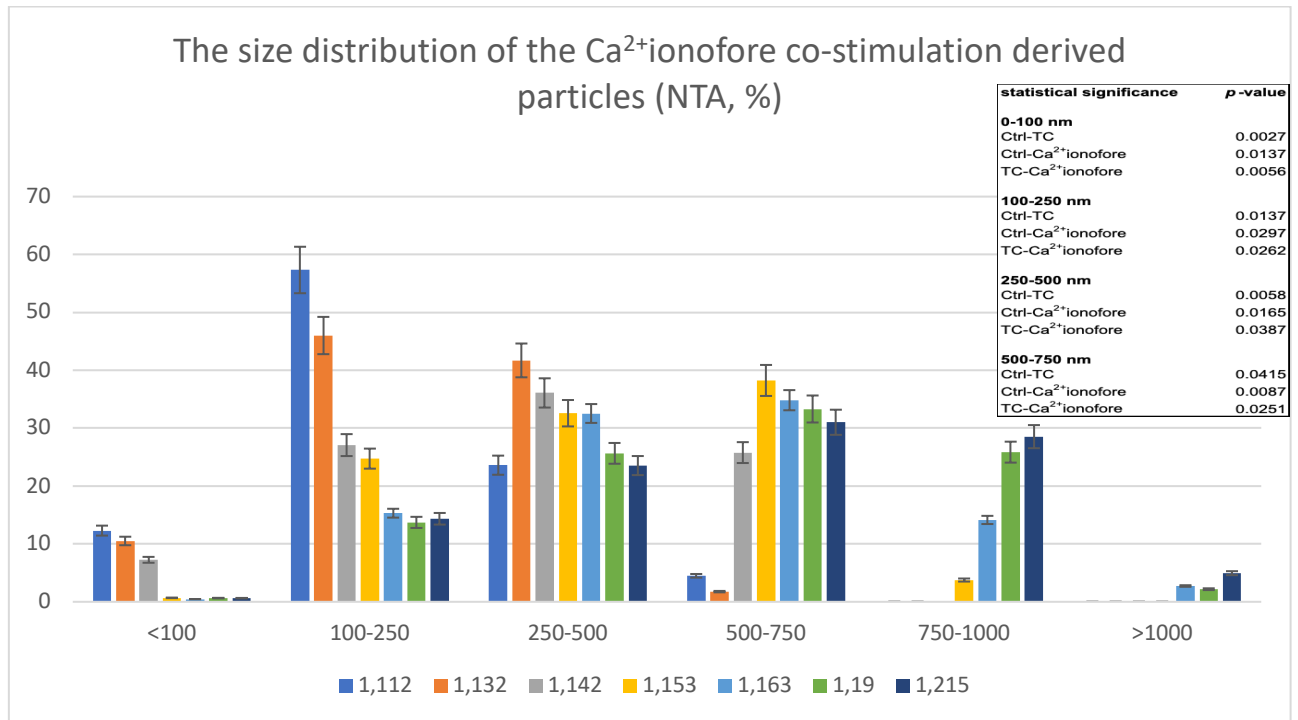


Figure 15 Density distribution and corresponding size of the particles derived from the stimulation by Ca²⁺ionofore. The density distribution of the particles within the different size groups were analysed by NTA. The density to diameter distribution appeared fairly similar to that of the TC co-stimulation. As a result of the Ca²⁺ionofore stimulation, however, the number of particles of smaller density was somewhat larger, effect of the unselective nature of the Ca²⁺ionofore stimuli.

The mean size distribution, of the samples derived from both the TC co-stimulus and the Ca²⁺ionofore stimulus, is displayed in the figure below (Figure 16). The variation in size depending on applied stimulus was not significant statistically. In all of the density groups, except for the particles with a density of 1.112 g ml⁻¹, the particles derived from the TC co-stimulus had the larger mean diameter compared to particles derived from stimulus by Ca²⁺ionofore.

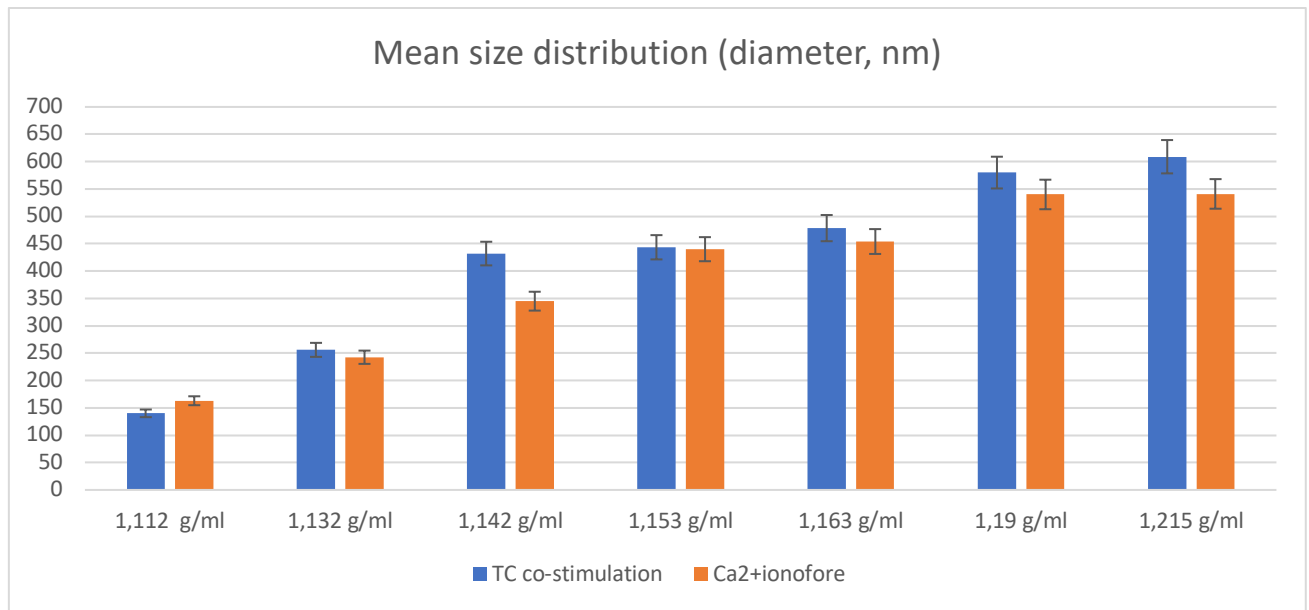


Figure 16 Comparison of the mean size distribution of the analysed particles. The applied stimulus on the density to diameter distribution does not appear statistically significant. Except for the particles with a density of 1.112 g ml⁻¹, the particles derived from the TC co-stimulus had the largest mean diameter.

4.3 Characterization of PEV by immunochemical methods

In this project the Western blot method was used in order to confirm a) that the isolated particles express EV typical cell-surface proteins and b) the expression of BDNF in the isolated particles. The expression of BDNF was further investigated by ELISA in order to gain both qualitative and quantitative data regarding the BDNF concentration in the particles.

4.3.1 Probing for the presence of EV surface markers on PEVs induced by TC/Ca²⁺ionofore activation

The presence of EV typical cell-surface proteins CD9 and CD63 in the PEV samples was investigated by Western blot. CD9 is a cell-surface glycoprotein that is a member of the tetraspanin family. It binds to integrins and modulates cell adhesion and cell migration (Chen et al. 1999). It also triggers platelet activation and aggregation. CD63 is also a member of the tetraspanin family that binds to integrins. It also forms complexes with intracellular vesicles and may also function as a marker for platelet activation (Cashicar and Hanson 2019).

The PEV samples derived from the TC co-stimulation and purified by density-gradient centrifugation showed a strong positive signal for CD9 at approximately 25 kDa (Figure 17). Iodixanol fractions 22%

(1.112 g ml⁻¹) and 24% (1.132 g ml⁻¹) showed the strongest signal. Fractions 26%-35% (1.142 g ml⁻¹-1.190 g ml⁻¹) were also positive, although the signal was not as strong. When probing for CD63, iodixanol fractions 22% (1.112 g ml⁻¹) and 24% (1.132 g ml⁻¹) also gave the strongest positive signals (Figure 18). Similar to CD9, fractions 26%-35% (1.142 g ml⁻¹-1.190 g ml⁻¹) also gave a weaker, yet positive signal (figure 18).

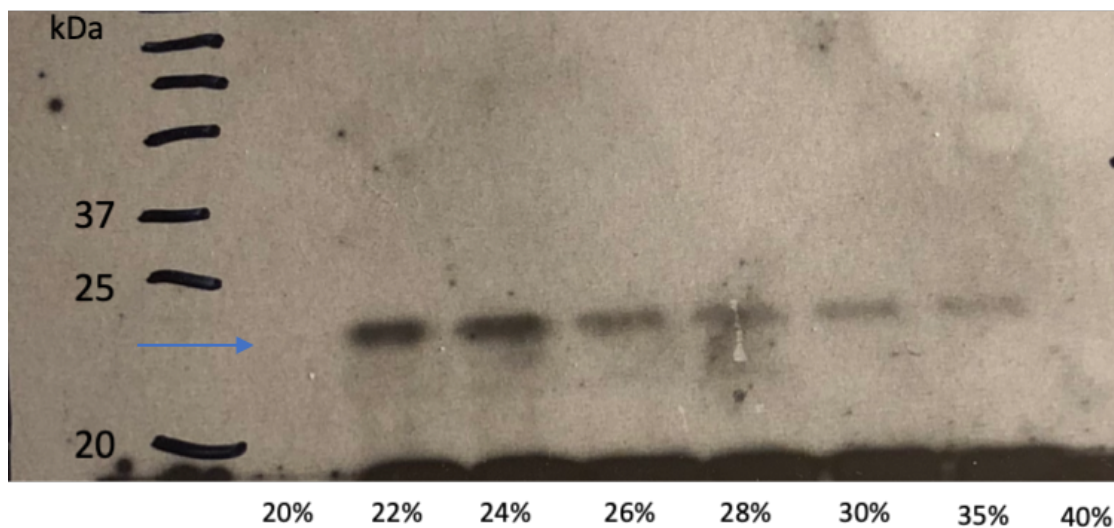


Figure 17 Western blot membrane probed with a CD9 antibody. The analysed sample was a TC co-stimulation derived PEV sample that was purified by density-gradient centrifugation. Fractions 35—22% (1.190 g ml⁻¹-1.112 g ml⁻¹) were positive for CD9, whereas fractions 40% (1.215 g ml⁻¹) and 20% (1.092 g ml⁻¹) were negative. The strongest signal was detected in fractions 22% and 24% The expected molecular weight for CD9 is approximately 25 kDa and it is indicated by an arrow. Results are representative of three repeats.

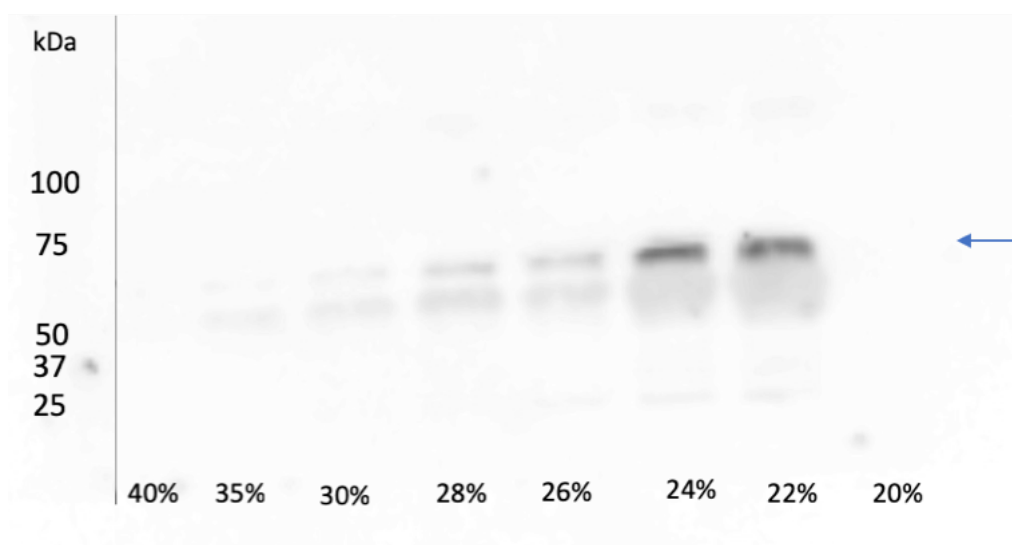


Figure 18 Western blot membrane probed with a CD63 antibody. The analysed sample was a PEV sample derived from TC co-stimulation was then purified by density-gradient centrifugation. Fractions 22%-35%

were positive for CD63 whereas fractions 40% and 20% were negative. Fractions 24% and 22% gave the strongest signal. The expected molecular weight for CD63 is approximately 65 kDa is indicated by an arrow. Data is representative of three repeats

Investigating the expression of BDNF in PEVs was a central aim of the project and as such the samples derived from the platelet activation were also probed for BDNF by Western blot analysis (Figure 19). In the figure the wells are marked with numbers and the corresponding samples are listed in the figure legend. The pre and post sec samples (sample 1 and 2) showed a strong positive signal at 11 kDa. There was also plenty of unspecific binding. The PEV sample derived from the TC co-stimulation (sample 4) was positive. The PEVs derived from the Ca²⁺ionofore activation (sample 5) were BDNF negative. As expected, the platelet samples that were left inactivated during the activation process (sample 6) were BDNF negative. This sample can be considered as a negative control. The brain lysate sample from mouse that was used as a positive control (sample 9) only gave a very faint signal although we pipetted approximately 50 µg of it onto the gel. The same amount of the brain lysate used as a negative control was pipetted on to the gel (sample 8) and it appears BDNF negative.

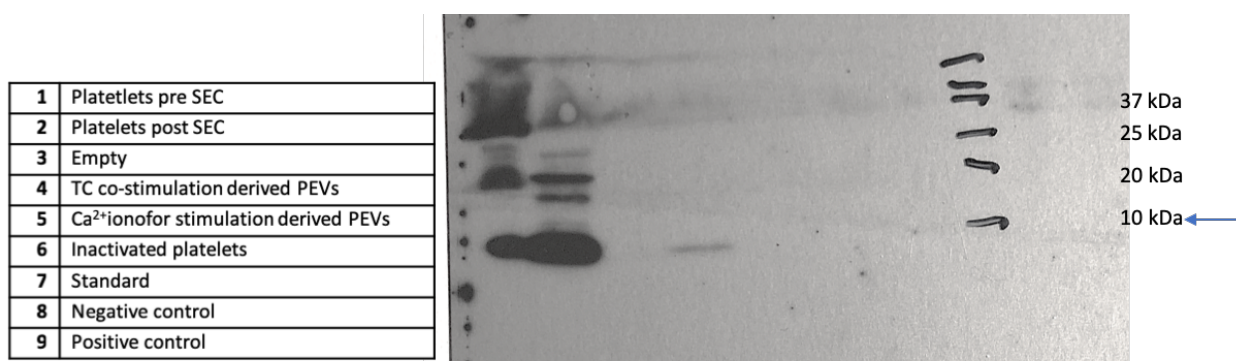


Figure 19 Western blot probed for BDNF. The highly positive signals in lane 1 and 2 are platelet samples pre- and post- isolation by size exclusion chromatography. The sample in lane 4 is TC co-stimulation-derived PEVs. The Ca²⁺ionofore-derived PEVs in lane 5 were negative as were the unactivated PEV samples in lane 6. The positive control of mouse brain lysate in lane 9 gave a very faint positive signal visible only with overexposure of the gels. The expected molecular weight of BDNF is approximately 11 kDa is indicated by an arrow. Results are representative of three repeats.

The PEVs purified by density-gradient centrifugation were also probed for BDNF by Western blot analysis. Based on the results, BDNF was enriched in fractions 22% and 24%, the latter giving the stronger positive signal (Figure 20). These fractions correspond to densities 1.112 g ml⁻¹ and 1.132 g ml⁻¹. The other fractions appeared to be BDNF negative even at longer exposures (data not shown).

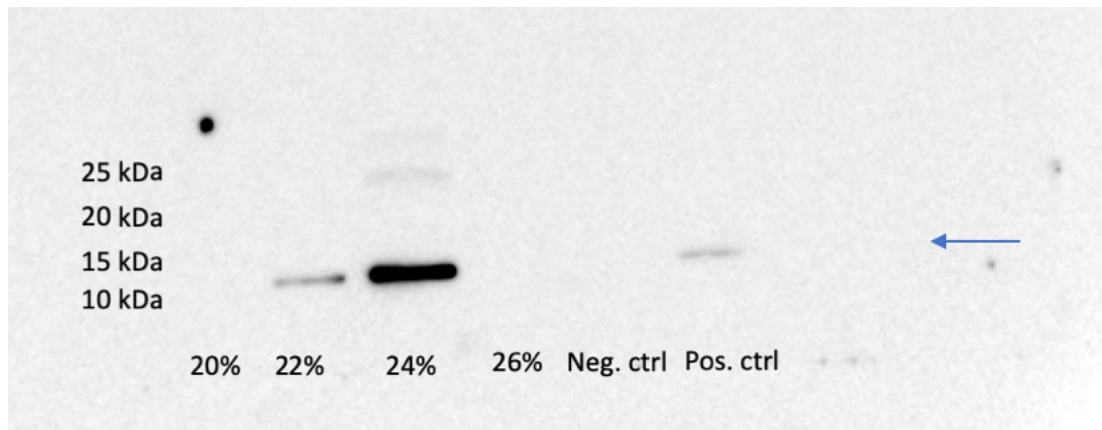


Figure 20 Western blot probed for BDNF. TC co-stimulation derived PEVs were purified by density-gradient centrifugation. Fractions 22% and 24% were positive for BDNF whereas the other fractions appeared to be BDNF negative. Results are representative of three repeats. The expected molecular weight of BDNF is approximately 11 kDa is indicated by an arrow

4.3.2 ELISA analysis

Once we had confirmed the presence of BDNF in our PEV samples we proceeded to analysis by ELISA, in order to obtain quantitative data. During the project, two ELISA analyses were run. For this first analysis we used the same sample volumes of PEVs as we did for the Western blot analysis. We chose to use the same samples undiluted since BDNF concentrations in PEVs had not previously been determined. In other words, there were no reference amounts available to proceed by. It turned out, however, that the samples were too concentrated for the ELISA since it is a more sensitive analysis. For the second ELISA (Figure 20) we made a dilution series where every sample was diluted 1/3 from the previous one. By doing so we ensured that our absorbance rates were within linear range of our BDNF standard curve.

The PEVs resulting from the TC co-stimulation contained the highest amount of BDNF relative to the total protein concentration of the samples analysed (Figure 21). Somewhat surprisingly the PEVs resulting from the Ca^{2+} -ionophore activation also contained some BDNF relative to the total protein concentration (Figure 21). The inactivated samples also contained BDNF (Figure 21). However, the amount normalised to the total protein concentration was only 33% compared to that of the PEVs derived from the TC co-stimulation. The platelet samples that we reused as positive controls also contained a lot of BDNF (Figure 21).

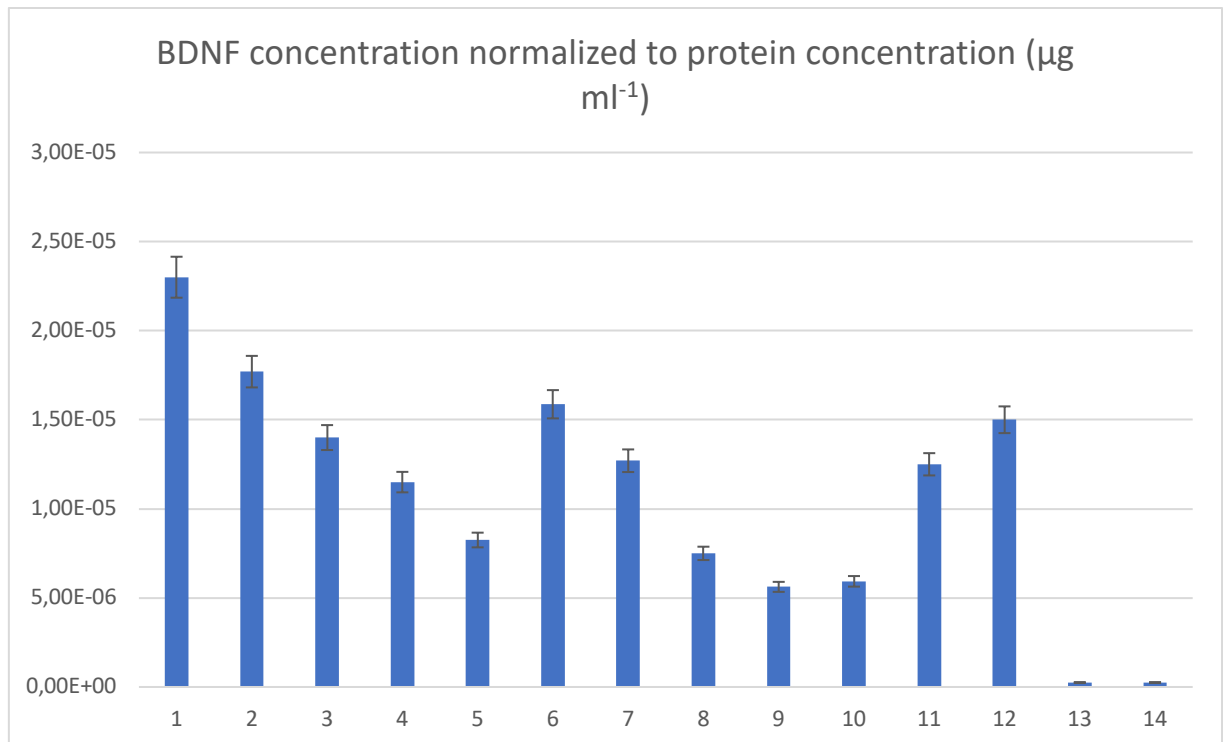


Figure 21 Figure displaying the BDNF-concentration in the PEV samples when normalized to protein concentration. Samples 1-5 are TC co-stimulation-derived PEVs as a dilution series. Samples 6-9 are Ca²⁺ionofore co-stimulation-induced PEVs as dilution series. Both sample types were diluted such that the next sample is diluted 1/3 in relation to the previous one. Sample 10 is the unactivated sample, samples 11 and 12 are platelet samples pre- and post- isolation by size exclusion chromatography. Sample 13 is the negative control and sample 14 is the positive control. Data is representative of three measurements.

Further we also wanted to analyse the BDNF concentration in relation to the particle concentration measured by NTA (Figure 22). When normalising the BDNF concentration to the particle amount the platelet control contained 0,263 pg particle⁻¹. The PEVs from the TC co-stimulation contained 0.46 pg particle⁻¹ and the PEVs from the Ca²⁺ionofore stimulation contained 0.053 pg particle⁻¹. This was expected due to the protein poor content of Ca²⁺ionofore induced EVs as shown by Aatonen et al. 2014.

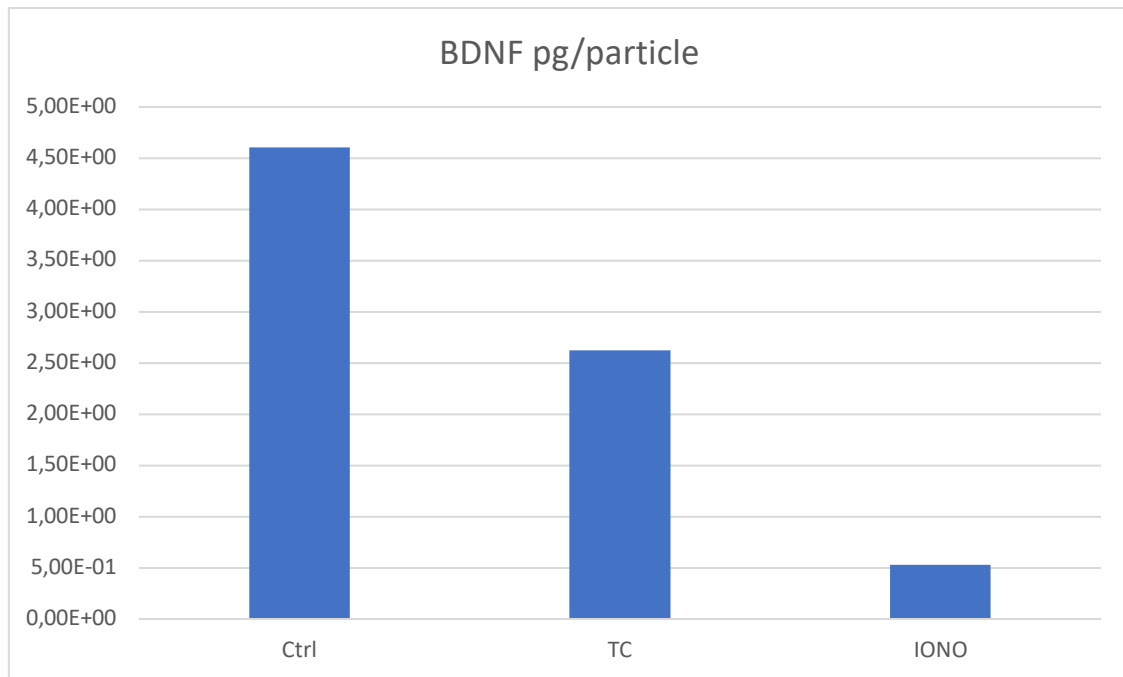


Figure 22 Analysis of BDNF concentration/particle measured by NTA. In the PEV samples we found that the control sample contained 0.263 pg BDNF particle⁻¹ whereas the particles derived from the TC co-stimulation contained 0.46 pg particle⁻¹. The CA²⁺ ionophore stimulation derived particles in the other hand contained 0.053 pg particle⁻¹.

5. Discussion

To ensure the reliability and reproducibility of EV related research, it is paramount that the analytical methods chosen compliment and reinforce each other. Also, to meaningfully claim that the results are EV-related and not co-isolate-related, we also need to evaluate the chosen methods critically. In the following, I want to address the analytical results of this study and to discuss the obtained results in the light of current EV-research. The fact that the obtained results are based on very few repeats (n) needs to be taken into consideration and as such conclusions should not be drawn lightly.

5.1 Flow cytometry

In this project, we wanted to investigate the BDNF-content in PEVs and further if the means of activation has an effect on the BDNF concentration or if it localizes into certain subpopulations. For this purpose, we stimulated the platelets in order for them to secrete PEVs. For the success of the project, it was important to know, with certainty, that the analysed PEVs were the result of agonist stimulation.

Based on the data from the flow cytometry, it is safe to say that the platelets treated with agonists had indeed become activated and that they secreted particles. As the control samples had remained largely inactive, it is also safe to say that the platelet activation was a result of the agonist treatment and not of careless platelet handling, for instance. The flow cytometry also confirmed that we were analysing PEVs since the inactivated particles were CD41 positive.

5.2 Immunochemical methods

PEVs derived from platelet activation were analysed by both Western blot and ELISA. By Western blot we confirmed the presence of typical EV proteins, such as CD9 and CD63. The expression of the platelet- and PEV-specific protein CD41 was confirmed by flow cytometry. The expression of CD9 and CD63 was confirmed by Western blot for both TC co-stimulation-derived PEVs and Ca^{2+} ionophore stimulation-derived PEVs. The expression of these proteins was also confirmed for the samples purified by density-gradient centrifugation. The several bands appearing on the Western blot probed for CD63 was due to the fact that CD63 has several isoforms i.e. it is not due to unspecific binding for instance. It is also worth noting that there, as of yet, does not exist an internal loading control for PEVs. This is why we probed for EV typical markers when aiming to verify the presence of PEVs. This is one example highlighting the need to verify EV related results from several angles.

As both CD9 and CD63 are members of the tetraspanins superfamily also analysing the PEVs for other EV typical markers would have been commendable (Théry 2018). The guidelines for qualitative EV-research are comprehensively discussed in the Minimal Information for Studies in Extracellular Vesicles (MISEV) (Théry et al. 2018). The tumour susceptibility gene 101, also known as TSG101, for instance is a cytosolic protein and not a membrane associated one such as CD9 and CD63. Thus, adding it to the analysis would have provided more solid proof for claiming that the isolated particles were indeed PEVs. Since there, as of yet, is no internal loading control for EVs it is recognised that several EV typical markers should always be probed for when analysing EVs immunochemically. ISEV also recommends verifying the presence of transmembrane proteins or lipid-bound extracellular proteins and cytosolic proteins in EV samples as negative controls (Théry et al. 2018). Since several comprehensive studies in PEV proteins had previously been carried out in the laboratory of Siljander it was not viewed as necessary for this particular study to perform a more extensive verification, however. Also, since we were interested in seeing whether the BDNF is soluble or EV-cargo we only performed a very rudimentary Western blot without quantification of protein bands and Ponceau S staining.

For a more thorough analysis it would also have been beneficial to analyse the samples for the plasma protein apolipoprotein B (Apo B). ApoB is the most common marker for chylomicrons - low density lipoprotein and very low-density lipoproteins. ApoB often co-isolates with the EVs of plasma and serum and it is regarded as one of the best negative controls when investigating PEVs (Théry et al. 2018). Based on possible ApoB-content we would have been able to assess the purity of our samples and thus the reliability of our results. Density-gradient ultracentrifugation is one of the methods by which the EV community hopes to get samples free from contaminants. It is, however, a recognized problem that this method has a very low yield and that soluble proteins remain as challenging contaminants (Karimi et al. 2018).

The main objective of the project was the BDNF cargo of PEVs. When probing for BDNF by Western blot the weakness of positive control i.e. the brain lysate of a knock-out mouse became a challenge. We only managed to get a signal from the positive control when probing for BDNF in PEVs purified by density-gradient ultracentrifugation (Fig. 23). This weakness may have been caused by aging of the sample or storage related issues. As it was known that platelets contain BDNF the pre- and post-sec samples were also expected to contain plenty of BDNF (Fujimura 2002). This was indeed confirmed by Western blot analysis. In other words, this positive control worked. The several protein bands appearing on the blot are likely to be isoforms of BDNF. The PEVs derived from the TC co-stimulation were positive for BDNF as well according to the Western blot analysis. This result was in line with earlier publications (Fujimura et al. 2002, Aatonen et al. 2014). The fact that the signal was significantly weaker than the signal from the pre- and post-sec is unsurprising. After all we did not aim on loading the same amounts of protein on to the gel, since we did not know what the EV to total protein concentration in the samples was. Also, from previous research we knew that the distribution of BDNF between the platelet cytoplasm and the alfa-granule is 70:30 (Fujimura et al 2002, Tamura et al. 2011) and further that the BDNF within the alfa-particles is secreted upon activation and the rest of the BDNF remains within the cytoplasm of the platelet (Tamura et al. 2011). Thus, the amount of BDNF within the platelet is likely to be significantly larger than that of the PEV (cytosolic). Based on the Western blot the PEVs derived from the Ca^{2+} ionophore stimulation appeared to be void of BDNF-content. However, based on both the results in this project and results from previous studies (Aatonen et al. 2014) it is known that Ca^{2+} ionophore stimulation of platelets produces a large population on PEVs that are relatively protein poor and thus this result alone was not enough in order to call these PEVs BDNF-negative.

Indeed, the ELISA analysis, which is more sensitive than Western blot, confirmed that the Ca^{2+} ionophore stimulation derived PEVs did contain BDNF. When analysing the results however, it became clear that even though the BDNF concentration in relation to the total protein concentration appeared promising, the BDNF concentration per particle was in fact miniscule. Supporting the Western blot finding the BDNF concentration of the Ca^{2+} ionophore stimulation derived PEVs was roughly 1/5 compared to that of the TC co-stimulation derived PEVs. As the BDNF concentration was normalised to protein content the PEVs derived from the TC co-stimulation were richer in BDNF than the other samples, including the platelets. Again, it must be kept in mind that we did not load equal amounts of protein for the ELISA analysis. For the first ELISA analysis we loaded equal volumes of the samples as we had loaded for the Western blots and for the second, we made a dilution series of our samples. Ideally, there would have been more time to optimize the method and the subsequent results would then be more than indicative as is the case now.

5.3 Determining of BDNF location in PEVs

By isolating the PEVs by differential centrifugation we had hoped to define in which PEV subfraction the BDNF rich PEVs were localized. Unfortunately, most likely due to sample loss, the fractions we analysed by ELISA all appeared to be BDNF negative (data not shown). Fortunately, we were able to confirm by Western blot that there were in fact BDNF positive fractions namely, fractions 22% and 24% of the TC co-stimulated samples. In other words, we know that the method works and that BDNF does localise in the subfractions where exosomes are expected to localise (Onódi et al. 2018). The samples analysed by Western blot which indicated that fractions 22% and 24% were BDNF positive and the ELISA which indicated otherwise where not the result of the same PEV isolation. In other words, it is quite possible that a new analysis would provide us with another kind of result.

The PEV-yield of the density-gradient centrifugation (17%) was not great, although within the limits provided by literature. Based on published literature the gain for EVs isolated by density-gradient centrifugation is between 10% and 50% (Coumans et al. 2017). The sample loss was probably, at least in part, due to the final step of the protocol where the fractions from the density-gradient centrifugation were collected, diluted 1:20 in HEPES buffer, ultracentrifugation, and resuspended in HEPES buffer in order to get rid of the iodixanol. By using a larger or more concentrated sample amount in the beginning of the density-gradient centrifugation, the yield is most likely to be improved. Also, obviously, having more time, to optimize the method and improve the technical skills of the person

performing the experiment, would minimize the sample loss and make the whole process more efficient.

5.4 Determining the size distribution of particles derived from activated platelets

When analysing the properties of the particles derived from the activated platelets by NTA we saw that both the size-distribution and the particle concentration, more or less, corresponded to the results acquired in the lab before (Aatonen et al. 2014). The particle concentration did not increase dramatically when activating platelets by TC co-stimulation as compared to the control sample. The protein content, however, was higher in the particles activated by TC co-stimulation than in the control sample. The particles derived from the platelets that were activated by Ca^{2+} ionophore, on the other, were greater in number as compared to both the control sample and the particles derived from the TC co-stimulation. Meanwhile, they were quite protein-poor. This tells us that platelets pack proteins into PEV based on the signal they receive. Ca^{2+} ionophore being a very general platelet activating agonist mainly produces vesiculation, whereas TC co-stimulation produces a selective packing of proteins into EVs as

Based on combined results from both Western blot, ELISA and NTA there appears to be enrichment of BDNF in the 22% and 24% density-gradient fractions. This corresponds to particles that have a density of 1.112 g ml^{-1} and 1.132 g ml^{-1} correspondingly. For particles derived from the TC co-stimulation these densities imply that the particles are less than 500 nm in diameter. The majority of the particles with a density of 1.112 g ml^{-1} correspond to particles with a diameter of 100-250 nm. This was also the size group with the largest particle concentration. The particles with a density of 1.132 g ml^{-1} were divided fairly equally between the groups with a diameter of 100-250nm and 250-500nm. Unfortunately, we do not have data for the density centrifuged samples of Ca^{2+} ionophore stimulation derived particles. This is most likely caused by the combination of sample loss and the protein poor nature of these particles.

5.5 Conclusions

What makes PEVs, and EVs in general, such a fascinating field of study is the fact that they participate in such a broad array of physiological and pathophysiological processes and these processes can be contradictory, from time to time. As such, intercellular communication is, in part, based on the

formation of a functionally diverse population of EVs that are produced by the cells for a specific function.

We set out to confirm our previous observations by mass spectrometry that BDNF is secreted into PEVs. We also wanted to investigate what kind of effect the means of activation had on the BDNF-content and the localization of BDNF into the PEV subpopulations. The data presented in this thesis affirms the active secretion of BDNF into PEVs derived from TC co-stimulation. This implies that BDNF is secreted into PEVs as a thrombogenic response, for instance in coronary heart disease (Amadio et al. 2019). Lower concentrations of peripheral BDNF concentrations are associated with bigger clots and greater fibrin clot strength and higher fibrin fiber complexity, when compared to healthy control subjects (Amadio et al. 2019). As such, BDNF may be of potential both as a biomarker and as a therapeutic agent for patients suffering from coronary heart disease. The fact that cargo is selectively and specifically packed into EVs is supported by published results as reviewed extensively, for instance by, Anand et al. and Margolis and Sadovsky (Anand et al. 2019, Margolis and Sadovsky 2019). As a further endeavour, it would be interesting to look deeper into how other platelet agonists might affect the BDNF content. It would be interesting to analyse and concentrate the supernatant to measure the amount, if any, of BDNF in the supernatant.

During the project we worked on trying to develop a method for isolating contaminant free PEVs. We also wanted to isolate PEVs based on their density. The method proved to be laborious and time-consuming. A further downside was the low gain which, at least in part, was due to sample loss. The purpose of isolating PEVs based on their density was to see whether platelet-derived BDNF localises in specific PEV subgroups or not. Based on our results BDNF seems to localise in platelets with a density of 1.112 g ml^{-1} and 1.1132 g ml^{-1} . In other words, BDNF seems to localise in the so-called exosome fraction. When verified, this information is useful when, for example, developing BDNF related therapeutic drug delivery systems (Gudbergsson et al. 2019). Further evidence for the success of the developed method was the fact that the isolated PEVs did separate in different fractions of the iodixanol gradient based on their densities and remained functional. The method needs further refinement, however.

BDNF is unable to cross the blood-brain barrier and it also has a short half-life (Wurzelmann et al. 2017). EVs, on the other hand have been shown to cross the blood-brain barrier (Saeedi et al. 2019). As they resist complement-mediated lysis (Clayton et al. 2003) EVs thus have the ability to shield their cargo and cross the blood-brain barrier. Further and comprehensive study is needed but by this logic

there is potential in employing EV as therapeutic agents in BDNF-related neural disorders. Peripheral BDNF, on the other hand, is hypothesised to have great potential as a biomarker when diagnosing and treating depression and coronary heart disease (Serra-Millá 2016, Amadio et al. 2019). It must, however, be taken into consideration that standardised methods for handling of BDNF as a reliable biomarker do, as of yet, not exist.

In conclusion, BDNF is central to several physiological and pathophysiological processes. The results presented in this thesis are encouraging for future research of what the adaptations of BDNF packed PEVs might have to offer. Much more research is necessary but at the same time further research will potentially result in new, exciting and meaningful discoveries regarding PEVs, peripheral BDNF and our health.

6. Acknowledgements

I want to express my deepest thanks to my supervisors Pia Siljander and Mari Palviainen. Their dedication to this project, their expertise and kindness is something I will be forever thankful for. This project coincided with an especially trying time in my life and the empathy that both Pia and Mari expressed, while at the same time pushing me forward, is invaluable.

I also want to thank Maarit Takatalo-Laine and Maarit Neuvonen for helping me in the lab whenever I needed it. A special thank you to Eero Castrén and his group for allowing me to work in his lab and providing me with the necessary material for experiments as well as invaluable advice.

Finally, I want to thank Hanna without whom I would never had ventured into biochemistry in the first place. To be lucky enough to have someone always by my side cheering me on and stopping me from throwing my computer into the wall is golden.

7. References

- Aatonen, M., Grönholm, M., Siljander, P. (2012). Platelet-derived microvesicles: Multitalented participants in intercellular communication. *Seminars in Thrombosis and Hemostasis*, doi: 10.1055/s-0031-1300956.
- Aatonen, M. T., Ohman, T., Nyman, T. A., Laitinen, S., Grönholm, M., & Siljander, P. (2014). Isolation and characterization of platelet-derived extracellular vesicles. *Journal of extracellular vesicles*, doi:10.3402/jev.v3.24692
- Aghaloo, T., Moy, P., Freymiller, E. (2002). Investigation of platelet-rich plasma in rabbit cranial defects: A pilot study. *Journal of Oral and Maxillofacial Surgery*, doi: <https://doi.org/10.1053/joms.2002.34994>
- Ambrosio, A.L, Di Pietro, S.M. (2017) Storage pool diseases illuminate platelet dense granule biogenesis. *Platelets*. doi: 10.1080/09537104.2016.1243789.
- Ali, R.A., Wuescher, L.M., Worth, R.G. (2015) Platelets: essential components of the immune system. *Current Trends in Immunology*;16, 65-78.
- Ananand, S., Samuel, M., Kumar, S., Mathivananan, S. (2019). Ticket to a bubble ride: Cargo sorting into exosomes and extracellular vesicles. *Biochimica et Biophysica Acta (BBA) - Proteins and Proteomics*, doi: 10.1016/j.bbapap.2019.02.005
- Akers, J. C., Gonda, D., Kim, R., Carter, B. S., and Chen, C. C. (2013). Biogenesis of extracellular vesicles (EV): exosomes, microvesicles, retrovirus-like vesicles, and apoptotic bodies. *Journal of neuro-oncology* 113, 1-11.
- Al-Nedawi, K., Meehan, B., and Janusz Rak, J. (2009) Microvesicles: Messengers and mediators of tumor progression, *Cell Cycle*, doi: 10.4161/cc.
- Alvarez-Erviti, L., Seow, Y., Yin, H.F., Betts, C., Lakhali, S. et al. (2011). Delivery of siRNA to the mouse brain by systemic injection of targeted exosomes. *Nature Biotechnology* 29, 341–345
- Amadio, P., Porro, B., Sandrini, L., Fiortelli, S., Bonomi, S. et al. (2019). Patho- physiological role of BDNF in fibrin clotting. *Scientific Reports*, doi:10.1038/s41598-018-37117-1
- Antwi-Baffour, S., Adjei, J., Aryeh, C., Kyeremeh, R., Kyei, F., & Seidu, M. A. (2015). Understanding the biosynthesis of platelets-derived extracellular vesicles. *Immunity, inflammation and disease*, doi: 10.1002/iid3.66

- Arraud, N, Linares, R, Tan, S, Gounou, C, Pasquet, J-M, Mornet, S, Brisson, AR. (2009). Extracellular vesicles from blood plasma: determination of their morphology, size, phenotype and concentration. *Journal of Thrombosis and Haemostasis* 12, 614–27
- Baaten, C., Cate, H., Meijdena, P., Heemskerk, J. (2017), Platelet populations and priming in hematological diseases. *Blood Reviews*, 31, 389-399
- Barde, Y. A., Edgar, D., and Thoenen, H. (1982). Purification of a new neurotrophic factor from mammalian brain. *The EMBO journal*, 1, 549-53.
- Barry OP., FitzGerald GA. (1999). Mechanisms of cellular activation by platelet microparticles. *Thrombosis and Haemostasis* 82, 794–800.
- Bebelman, M., Smit, M., Pegtel, M., Baglio, R. (2018). Biogenesis and function of extracellular vesicles in cancer. *Pharmacology & Therapeutics*, doi: 10.1016/j.pharmthera.2018.02.013
- Bibel M and Barde YA (2000). Neurotrophins: key regulators of cell fate and cell shape in the vertebrate nervous system. *Genes and Development*. 14,2919–2937
- Bobrie, A., Krumeich, S., Rey, F., Recchi, C., Moita, L. (2012). Rab27a Supports Exosome-Dependent and -Independent Mechanisms That Modify the Tumor Microenvironment and Can Promote Tumor Progression. *Cancer Research*, doi: 10.1158/0008-5472.CAN-12-0925
- Blair P, Flaumenhaft R. (2009) Platelet alpha-granules: basic biology and clinical correlates. *Blood Reviews*, doi: 10.1016/j.blre.2009.04.001.
- Cashikar, A. G., and Hanson, P. I. (2019). A cell-based assay for CD63-containing extracellular vesicles. *PloS one*, doi:10.1371/journal.pone.0220007
- Castrén, E. and Lindholm, D. (1992). Hermokasvutekijän reseptorin arvoitus selviämässä. *Duodecim*, 108, 10-10
- Chacón-Fernández, P., Säuberli, K., Colzani, M., Moreau, T., Ghevaert, C. and Barde, Y. A. (2016). Brain-derived Neurotrophic Factor in Megakaryocytes. *The Journal of biological chemistry*, 291, 9872-81.
- Chargaff, E. and West, R. (1946). The biological significance of the thromboplastic protein of blood. *Journal of biological Chemistry*, 166, 189-97
- Chen, M. S., Tung, K. S., Coonrod, S. A., Takahashi, Y., Bigler, D., Chang, A., ... White, J. M. (1999). Role of the integrin-associated protein CD9 in binding between sperm ADAM 2 and the egg integrin alpha6beta1: implications for murine fertilization. *Proceedings of the National Academy of Sciences of the United States of America*, doi:10.1073/pnas.96.21.11830

- Choi, D. , Park, J. O., Jang, S. C., Yoon, Y. J., Jung, J. W., Choi, D. , Kim, J. , Kang, J. S., Park, J. , Hwang, D. , Lee, K. , Park, S. , Kim, Y. , Desiderio, D. M., Kim, K. P. and Gho, Y. S. (2011), Proteomic analysis of microvesicles derived from human colorectal cancer ascites. *Proteomics*, doi:10.1002/pmic.201100022
- Chow, A., Zhou, W., Liu, L., Fong, M., Champer, J. (2014). Macrophage immunomodulation by breast cancer-derived exosomes requires Toll-like receptor 2-mediated activation of NF- κ B. *Scientific Reports*, doi: 10.1038/srep05750
- Clayton, A. Al-Taei, S., Webber, J., Mason, M., Tabi, Z. (2011). Cancer Exosomes Express CD39 and CD73, which Suppress T Cells through Adenosine Production. *Journal of Immunology* 187, 676-683
- Comelli, L., Rocchiccioli, S., Smirni, S., Salvetti, A., Signore, G. (2014). Characterization of secreted vesicles from vascular smooth muscle cells. *Molecular BioSystems*, doi: 10.1039/c3mb70544g.
- Coumans, F. Brisson, A., Buzas, E., Dignat-George, F., Drees, E. (2017). Methodological Guidelines to Study Extracellular Vesicles. *Circulation Research*, doi:10.1161/CIRCRESAHA.117.309417
- Curtis, A. M., Edelberg, J., Jonas, R., Rogers, W. T., Moore, J. S., Syed, W., & Mohler, E. R. (2013). Endothelial microparticles: sophisticated vesicles modulating vascular function. *Vascular medicine* (London, England), doi:10.1177/1358863X13499773
- Davila, M., Amirkhosravi, A., Coll, E., Desai, H., Roles, L., et al. (2008), Tissue factor-bearing microparticles derived from tumor cells: impact on coagulation activation. *Journal of Thrombosis and Haemostasis*, 6, 1517-1524
- Delabranche X., Berger A., Boisrame-Helms J., Meziani F. (2012) Microparticles and infectious diseases. *Médecine et Maladies Infectieuses*, doi: 10.1016/j.medmal.2012.05.011
- Dechant, G., Biffo, S., Okazawa, H., Kolbeck, R., J. Pottgiesser, J., Barde, Y.A. (1993), *Development*, 119, 545-558
- de Vooght, K., Lau, C., de Laat, P., van Wijk, R., van Solinge, W., Schiffelers, R. (2013). Extracellular vesicles in the circulation: are erythrocyte microvesicles a confounder in the plasma haemoglobin assay? *Biochemical Society Transactions*, doi: 10.1042/BST20120254
- Duchez, A. C., Boudreau, L. H., Naika, G. S., Bollinger, J., Belleannée, C., et al. (2015). Platelet microparticles are internalized in neutrophils via the concerted activity of 12-lipoxygenase and secreted phospholipase A2-IIA. *Proceedings of the National Academy of Sciences of the United States of America*, doi: 10.1073/pnas.1507905112
- Gudbersson, J, Jønsson, K., Simonsen, J., Johnsen, K. (2019). Systematic review of targeted extracellular vesicles for drug delivery – Considerations on methodological and biological heterogeneity. *Journal of Controlled Release*, doi: 10.1016/j.jconrel.2019.06.006

- Herr, N., Bode, C., & Duerschmied, D. (2017). The Effects of Serotonin in Immune Cells. *Frontiers in cardiovascular medicine*, doi:10.3389/fcvm.2017.00048
- Ernfors, P., Wetmore, C., Olson, L., Persson, H. (1990). Identification of cells in rat brain and peripheral tissues expressing mRNA for members of the nerve growth factor family. *Neuron*, doi: 10.1016/0896-6273(90)90090-3
- Escolar, G., Leistikow, E., and White, J. (1989). The fate of the open canalicular system in surface and suspension- activated platelets. *Blood*, 74, 1983-1988
- Flaumenhaft, R., Dilks, J. R., Richardson, J., Alden, E., Patel-Hett, S. R., et al. (2009). Megakaryocyte-derived microparticles: direct visualization and distinction from platelet-derived microparticles. *Blood*, 113, 1112-21.
- Frojmovic, M. and Milton, J. (1982) Human platelet size, shape, and related functions in health and disease. *Physiological Reviews* 62,185-261
- Fujimura, H., Altar, C.A., Chen, R., Nakamura, T., Nakahashi, T., Kambayashi, J. (2002). Brain-derived neurotrophic factor is stored in human platelets and released by agonist stimulation. *Thrombosis and haemostasis*, 87, 728-34.
- Gao, X., Ran, N., Dong, X., Zuo, B., Yang, R. (2018). Anchor peptide captures, targets, and loads exosomes of diverse origins for diagnostics and therapy. *Science Translational Medicine*. doi: 10.1126/scitranslmed.aat0195
- George, S., Nagabhushana, M. S. and Cyran, E. M. (1995), Coagulopathy due to an acquired factor V inhibitor and subsequently thrombosis. *American Journal of Hematology.*, doi:10.1002/ajh.2830490122
- Golebiewska, E. M., & Poole, A. W. (2015). Platelet secretion: From haemostasis to wound healing and beyond. *Blood reviews*, 29, 153-62.
- Gould, S. J., & Raposo, G. (2013). As we wait: coping with an imperfect nomenclature for extracellular vesicles. *Journal of extracellular vesicles*, doi:10.3402/jev.v2i0.20389
- Gue, Y.X., Gorog, D.A. (2017) Importance of Endogenous Fibrinolysis in Platelet Thrombus Formation. *International Journal of Molecular Sciences*, doi: 10.3390/ijms18091850.
- Guha, D., Mukerji, S., Chettimada, S., Misra, V., Lorenz, D., Morgello, S., Gabuzda, D. (2019). Cerebrospinal fluid extracellular vesicles and neurofilament light protein as biomarkers of central nervous system injury in HIV-infected patients on antiretroviral therapy. *AIDS*, doi: 10.1097/QAD.0000000000002121

Haggadone, MD. and Peters-Golden, M. (2018). Microenvironmental Influences on Extracellular Vesicle-Mediated Communication in the Lung. *Trends in Molecular Medicine*, doi: 10.1016/j.molmed.2018.08.006

Haimovich, G., Ecker, C. M., Dunagin, M. C., Eggan, E., Raj, A., Gerst, J. E., & Singer, R. H. (2017). Intercellular mRNA trafficking via membrane nanotube-like extensions in mammalian cells. *Proceedings of the National Academy of Sciences of the United States of America*, doi: 10.1073/pnas.1706365114

Harada, Y., Suzuki, T., Fukushige, T., Kizuka, Y., Yagi, H. (2019). Generation of the heterogeneity of extracellular vesicles by membrane organization and sorting machineries. *Biochimica et Biophysica Acta (BBA) - General Subjects*, doi: [10.1016/j.bbagen.2019.01.015](https://doi.org/10.1016/j.bbagen.2019.01.015)

Heijnen, HF., Debili, N., Vainchencker, W., Breton-Gorius, J., Geuze, H.J., Sixma, J.J. (1998) Multivesicular bodies are an intermediate stage in the formation of platelet alpha-granules. *Blood*, 91, 2313-2325

Heijnen, H. F., Schiel, A. E., Fijnheer, R., Geuze, H. J. and Sixma, J. J. (1999). Activated Platelets Release Two Types of Membrane Vesicles: Microvesicles by Surface Shedding and Exosomes Derived From Exocytosis of Multivesicular Bodies and Alfa-Granules. *Blood*, 94, 3791-3799

Jiang, L., Paone, S., Caruso, S., Atkin-Smith, G. K., Phan, T. K., Hulett, M. D., & Poon, I. (2017). Determining the contents and cell origins of apoptotic bodies by flow cytometry. *Scientific reports*, doi:10.1038/s41598-017-14305-z

Jiang, X. and Gao J-Q. (2017), Exosomes as novel bio-carriers for gene and drug delivery. *International Journal of Pharmaceutics*, doi: 10.1016/j.ijpharm.2017.02.038

Johnstone, RM, Bianchini, A and Teng. K. (1989). Reticulocyte maturation and exosome release: transferrin receptor containing exosomes shows multiple plasma membrane functions. *Blood* 74, 1844-1851

Kaneez, F. and Saeed, S. (2009). Investigating GABA and its function in platelets as compared to neurons. *Platelets*, doi: 10.1080/09537100903047752.

Kalra, H., Simpson, R. J., Ji, H., Aikawa, E., Altevogt, Pet al. (2012). Vesiclepedia: a compendium for extracellular vesicles with continuous community annotation. *PLoS biology*, doi: 10.1371/journal.pbio.1001450

Kalra, H., Drummen, G.P., Mathivanan, S. (2016). Focus on Extracellular Vesicles: Introducing the Next Small Big Thing. *International Journal of Molecular Sciences*, doi: 10.3390/ijms17020170.

Kaplan, D., Chao, F., Stiles, C., Antoniades, H., and Scher, C. (1979). Platelet alpha granules contain a growth factor for fibroblasts. *Blood*, 53, 1043-1052

Kapustin, A. N., & Shanahan, C. M. (2016). Emerging roles for vascular smooth muscle cell exosomes in calcification and coagulation. *The Journal of physiology*, doi: 10.1113/JP271340

Karimi, N., Cyjetkovic, A., Jang, S.C., Crescitelli, R., Hosseinpour Feizi, M.A. (2018). Detailed analysis of the plasma extracellular vesicle proteome after separation from lipoproteins. *Cell Molecular Life Sciences*. doi: 10.1007/s00018-018-2773-4

Kerschensteiner, M., Gallmeier, E., Behrens, L., Leal, V. V., Misgeld, T., et al. (1999). Activated human T cells, B cells, and monocytes produce brain-derived neurotrophic factor in vitro and in inflammatory brain lesions: a neuroprotective role of inflammation? *The Journal of experimental medicine*, 189, 865-70.

Kim, D. K., Kang, B., Kim, O. Y., Choi, D. S., Lee, et al. (2013). EVpedia: an integrated database of high-throughput data for systemic analyses of extracellular vesicles. *Journal of extracellular vesicles*, doi:10.3402/jev.v2i0.20384

Konoshenko, M., Lekchonov, E., Vlassov, A. and Laktionov, P. (2018). Isolation of Extracellular Vesicles: General Methodologies and Latest Trends. *Biomed research international*, doi: 10.1155/2018/8545347

Koupenova M, Clancy L, Corkrey HA, Freedman JE. Circulating Platelets as Mediators of Immunity, Inflammation, and Thrombosis. *Circulation Research*. doi: 10.1161/CIRCRESAHA.117.310795.

Kowiański, P., Lietzau, G., Czuba, E., Waśkow, M., Steliga, A., Moryś, J. (2018). BDNF: A Key Factor with Multipotent Impact on Brain Signaling and Synaptic Plasticity. *Cellular and Molecular Neurobiology* doi: 10.1007/s10571-017-0510-4.

Laffont, B., Corduan, A., Plé, H., Duchez, A., Cloutier, N., Boilard, E., and Provost, P. (2013). Activated platelets can deliver mRNA regulatory Ago2•microRNA complexes to endothelial cells via microparticles. *Blood*, 122, 253-261.

Lázaro-Ibáñez, E., Sanz-Garcia, A., Visakorpi, T., Escobedo-Lucea, C., Siljander, P., Ayuso-Sacido, Á. and Yliperttula, M. (2014), Different gDNA content in the subpopulations of prostate cancer extracellular vesicles: Apoptotic bodies, microvesicles, and exosomes. *Prostate*, doi:10.1002/pros.22853

Lefrançois, E. & Looney, M. (2019). Platelet Biogenesis in the Lung Circulation. *Physiology*, doi:10.1152/physiol.00017.2019

Lenassi, M., Cagney, G., Liao, M., Vaupotic, T., Bartholomeeusen, K., et al. (2010). HIV Nef is secreted in exosomes and triggers apoptosis in bystander CD4+ T cells. *Traffic (Copenhagen, Denmark)*, 11, 110-22.

- Levite, M. (2016). Dopamine and T cells: dopamine receptors and potent effects on T cells, dopamine production in T cells, and abnormalities in the dopaminergic system in T cells in autoimmune, neurological and psychiatric diseases. *Acta Physiologica*, doi:10.1111/apha.12476
- Lhermusier, T., Chap, H. and Payrastre, B. (2011), Platelet membrane phospholipid asymmetry: from the characterization of a scramblase activity to the identification of an essential protein mutated in Scott syndrome. *Journal of Thrombosis and Haemostasis*, doi:10.1111/j.1538-7836.2011.04478.x
- Lindsay, C., Edelstein, L. (2016). MicroRNAs in Platelet Physiology and Function. *Seminars in Thrombosis and Hemostasis*, doi: 10.1055/s-0035-1570077.
- Lood, C., Amisten, S., Gullstrand, B., Jönsen, A., Allhorn, M., Truedsson, L., Sturfelt, G., Erlinge, D., Bengtsson, A. A. (2010). Platelet transcriptional profile and protein expression in patients with systemic lupus erythematosus: up-regulation of the type I interferon system is strongly associated with vascular disease. *Blood*, 116, 1951-1957
- Iyer, S., and Acharya, K. R. (2011). Tying the knot: the cystine signature and molecular-recognition processes of the vascular endothelial growth factor family of angiogenic cytokines. *The FEBS journal*, 278, 4304-22.
- Laske, C., Stransky, E., Eschweiler, G.W., Maetzler, W., Wittorf, A. (2007). BDNF serum and CSF concentrations in Alzheimer's disease, normal pressure hydrocephalus and healthy controls. *Journal of psychiatric research*, doi: 10.1016/j.jpsychires.2006.01.014
- Ludány, A. and Kellerman, M. (1988). Protein synthesis in human platelets. *Clinical Biochemistry*, doi: 10.1016/S0009-9120(88)80097-3
- Lötvall, J., Hill, A. F., Hochberg, F., Buzás, E. I., Di Vizio, D., et al. (2014). Minimal experimental requirements for definition of extracellular vesicles and their functions: a position statement from the International Society for Extracellular Vesicles. *Journal of extracellular vesicles*, doi:10.3402/jev.v3.26913
- Ma, L., Hollenberg, M. and Wallace, J. (2001). Thrombin-induced platelet endostatin release is blocked by a proteinase activated receptor-4 (PAR4) antagonist. *British journal of pharmacology*, 134, 701-4.
- MacDonald N.Q., Lapatto, R., Murray-Rust, J., Gunning, J., Wlodawer, A. and Blundell, T.L. (1991) New protein fold revealed by a 2.3-Å resolution crystal structure of nerve growth factor. *Nature*, 354, 411–414
- MacDonald N.Q. and Hendrickson, W.A. (1993) A structural family of growth factors containing a cystine knot motif. *Cell*, 73, 421–424

- Maisonpierre, P., Le Beau, M., Espinosa, R., Belluscio, I., de la Monte, S. (1991). Human and rat brain-derived neurotrophic factor and neurotrophin-3: Gene structures, distributions, and chromosomal localizations. *Genomics*, doi: 10.1016/0888-7543(91)90436-I
- Malvezzi, M., Chalat, M., Janjusevic, R., Picollo, A., Terashima, H. (2013) Ca²⁺-dependent phospholipid scrambling by a reconstituted TMEM16 ion channel. *Nature Communications*, doi:10.1038/ncomms3367
- Mancek-Keber, M., Frank-Bertonceli, M., Hafner-Bratkovic, I., Smole, A., Zorko, M. (2015). Toll-like receptor 4 senses oxidative stress mediated by the oxidation of phospholipids in extracellular vesicles. *Science Signalling*, doi: 10.1126/scisignal.2005860
- Margolis L, Sadovsky Y (2019) The biology of extracellular vesicles: The known unknowns. *PLoS Biology*, doi: 0.1371/journal.pbio.3000363
- Martínez, C., Tesse, A., Zobairi, F., Andriantsitohaina, R. (2005). Shed membrane microparticles from circulating and vascular cells in regulating vascular function *American Journal of Physiology-Heart and Circulatory Physiology*, doi: 10.1152/ajpheart.00842.2004
- Mathieu, M., Martin-Jaular, L., Lavieu, G., Théry, C. (2019). Specificities of secretion and uptake of exosomes and other extracellular vesicles for cell-to-cell communication. *Nature Cell Biology*, doi: 10.1038/s41556-018-0250-9
- Meyers, K., Holmsten, H. and Seachord, C. (1982). Comparative study of platelet dense granule constituents. *American journal of physiology*, doi: 10.1152/ajpregu.1982.243.3.R454
- Maynard, D., Heijnen, H., Horne, M., White, J. G., and Gahl, W. (2007). Proteomic analysis of platelet α -granules using mass spectrometry. *Journal of Thrombosis and Haemostasis*, doi: 10.1111/j.1538-7836.2007.02690.x
- Monteleone, P., Fabrazzo, M., Martiadis, V., Serritella, C., Pannuto, M., and Maj, M. (2005). Circulating brain-derived neurotrophic factor is decreased in women with anorexia and bulimia nervosa but not in women with binge-eating disorder: Relationships to co-morbid depression, psychopathology and hormonal variables. *Psychological Medicine*, doi: 10.1017/S0033291704003368
- Onódi Z, Pelyhe C, Terézia Nagy C, Brenner GB, Almási L, et al. (2018) Isolation of High-Purity Extracellular Vesicles by the Combination of Iodixanol Density Gradient Ultracentrifugation and Bind-Elute Chromatography Blood Plasma. *Frontiers of Physiology*, doi: 10.3389/fphys.2018.01479.
- van Nispen tot Pannerden, H., de Haas, F., Geerts, W., Posthuma, G., van Dijk, S., and Heijnen, H. F. (2010). The platelet interior revisited: electron tomography reveals tubular α -granule subtypes. *Blood*, 116, 1147-1156

Piccin, A., Murphy, W., Smith, O. (2007). Circulating microparticles: pathophysiology and clinical implications. *Blood Reviews*, doi: [10.1016/j.blre.2006.09.001](https://doi.org/10.1016/j.blre.2006.09.001)

Protein Data Bank Europe, 12.5.2019, <https://www.ebi.ac.uk/pdbe/entry/pdb/1b8m/protein/1>

Ponomarev, E. (2018). Fresh Evidence for Platelets as Neuronal and Innate Immune Cells: Their Role in the Activation, Differentiation, and Deactivation of Th1, Th17, and Tregs during Tissue Inflammation. *Frontiers in immunology*, doi: [10.3389/fimmu.2018.00406](https://doi.org/10.3389/fimmu.2018.00406)

Pugholm, L. H., Bæk, R., Søndergaard, E. K., Revenfeld, A. L., Jørgensen, M. M., and Varming, K. (2016). Phenotyping of Leukocytes and Leukocyte-Derived Extracellular Vesicles. *Journal of immunology research*, doi: [10.1155/2016/6391264](https://doi.org/10.1155/2016/6391264)

Puhka, M., Takatalo, M., Nordberg, M. E., Valkonen, S., Nandania, J., et al. (2017). Metabolomic Profiling of Extracellular Vesicles and Alternative Normalization Methods Reveal Enriched Metabolites and Strategies to Study Prostate Cancer-Related Changes. *Theranostics*, doi: [10.7150/thno.19890](https://doi.org/10.7150/thno.19890)

Raap, U., Goltz, C., Deneka, N., Bruder, M., Renz, H. (2005). Brain-derived neurotrophic factor is increased in atopic dermatitis and modulates eosinophil functions compared with that seen in nonatopic subjects, doi: [10.1016/j.jaci.2005.02.007](https://doi.org/10.1016/j.jaci.2005.02.007)

Radley, J., and Haller, C. (1982). The demarcation membrane system of the megakaryocyte: a misnomer? *Blood*, 60, 213-219

Raimondo, S., Saieva, L., Corrado, C., Fontana, S., Flugy, A., Rizzo, A., De Leo, G., ... Alessandro, R. (2015). Chronic myeloid leukemia-derived exosomes promote tumor growth through an autocrine mechanism. *Cell communication and signaling*, doi:[10.1186/s12964-015-0086-x](https://doi.org/10.1186/s12964-015-0086-x)

Ratajczak, M. Z., and Ratajczak, J. (2016). Horizontal transfer of RNA and proteins between cells by extracellular microvesicles: 14 years later. *Clinical and translational medicine*, doi: [10.1186/s40169-016-0087-4](https://doi.org/10.1186/s40169-016-0087-4)

Rand ML, Wang H, Bang KW, Packham MA, Freedman J. (2006). Rapid clearance of procoagulant platelet-derived microparticles from the circulation of rabbits. *Journal of Thrombosis and Haemostasis* 4, 1621–3

Rank A, Nieuwland R, Crispin A, Grutzner S, Iberer M, et al. (2011). Clearance of platelet microparticles in vivo. *Platelets* 22, 111–16

Ray DM., Spinelli SL., Pollock SJ., Murant TI., O'Brien JJ, et al. (2008). Peroxisome proliferator-activated receptor gamma and retinoid X receptor transcription factors are released from activated human platelets and shed in microparticles. *Thrombosis and Haemostasis* 99, 86–95.

Pius-Sadowska, E. and Machaliński, B. (2017). BDNF – A key player in cardiovascular system. *Journal of Molecular and Cellular Cardiology*, doi: 10.1016/j.yjmcc.2017.07.007

Safaei R, Larson BJ, Cheng TC, Gibson MA, Otani S, Naerdemann W, Howell SB (2005). Abnormal lysosomal trafficking and enhanced exosomal export of cisplatin in drug-resistant human ovarian carcinoma cells. *Molecular Cancer Therapy* 4, 1595–1604.

Shedden, K., Xie, XT., Chandaroy, P., Chang, YT., Rosania, GR. (2003). Expulsion of small molecules in vesicles shed by cancer cells: Association with gene expression and chemosensitivity profiles. *Cancer Research* 63, 4331–4337

Schimizu, E., Hashimoto, K., Okamura, N., Koike, K., Kumakiri, K. (2003). Alterations of serum levels of brain-derived neurotrophic factor (BDNF) in depressed patients with or without antidepressants. *Biological Psychiatry*, doi: 10.1016/S0006-3223(03)00181-1

Schliephake H. (2002). Bone growth factors in maxillofacial skeletal reconstruction. *International Journal of Oral Maxillofacial Surgery*. doi: 10.1054/ijom.2002.0244.

Serra-Millàs M. (2016). Are the changes in the peripheral brain-derived neurotrophic factor levels due to platelet activation? *World Journal of Psychiatry*, doi:10.5498/wjp.v6.i1.84

Serra-Millàs, M., López-Vílchez, I., Navarro, V. (2011). Changes in plasma and platelet BDNF levels induced by S-citalopram in major depression. *Psychopharmacology*, doi: 10.1007/s00213-011-2180-0

Siljander, P. R.M. (2011). Platelet-derived microparticles – an updated perspective. *Thrombosis Research*, Volume 127, S30 - S33

Simpson, R., Kalra, H. and Mathivanan, S. (2012) ExoCarta as a resource for exosomal research, *Journal of Extracellular Vesicles*, doi: [10.3402/jev.v1i0.18374](https://doi.org/10.3402/jev.v1i0.18374)

Sonmez, O. and Sonmez, M. (2017). Role of platelets in immune system and inflammation. *Porto Biomedical Journal*. doi: [10.1016/j.pbj.2017.05.005](https://doi.org/10.1016/j.pbj.2017.05.005)

Starossom SC, Veremeyko T, Yung AW, Dukhinova M, Au C, Lau AY, Weiner HL, Ponomarev ED (2015) Platelets play differential role during the initiation and progression of autoimmune neuroinflammation. *Circulation Research* 117, 779–792.

Sveshnikova, A., Ataullakhanov, F., Panteleev, M. (2015). Compartmentalized calcium signaling triggers subpopulation formation upon platelet activation through PAR1. *Molecular BioSystems*, doi: [10.1039/C4MB00667D](https://doi.org/10.1039/C4MB00667D)

Tamura, S., Suzuki, H., Hirowatari, Y., Hatase, M., Nagasawa, A. (2011). Release reaction of brain-derived neurotrophic factor (BDNF) through PAR1 activation and its two distinct pools in human platelets. *Thrombosis Research*, doi: 10.1016/j.thromres.2011.06.002

Théry, C., Amigorena, S., Raposo, G. and Clayton, A. (2006), Isolation and Characterization of Exosomes from Cell Culture Supernatants and Biological Fluids. *Current Protocols in Cell Biology*, doi:10.1002/0471143030.cb0322s30

Théry, C., Witwer, K. W., Aikawa, E., Alcaraz, M. J., Anderson, J. D., et al. (2018). Minimal information for studies of extracellular vesicles 2018 (MISEV2018): a position statement of the International Society for Extracellular Vesicles and update of the MISEV2014 guidelines. *Journal of extracellular vesicles*. doi:10.1080/20013078.2018.1535750

Tkach, M. and Théry, C. (2016). Communication by Extracellular Vesicles: Where We Are and Where We Need to Go. *Cell*, doi: 10.1016/j.cell.2016.01.043

Todorova, D., Simoncini, S., Lacroix, R., Sabatier, F., Dignant-George, F. (2017). Extracellular Vesicles in Angiogenesis. *Circulation Research*, doi: 10.1161/CIRCRESAHA.117.309681

Umez, T., Tadokoro, H., Azuma, K., Yoshizawa, S., Ohyashiki, K., and Ohyashiki, J. H. (2014). Exosomal miR-135b shed from hypoxic multiple myeloma cells enhances angiogenesis by targeting factor-inhibiting HIF-1. *Blood*. doi: 10.1182/blood-2014-05-576116.

Vajen, T., Benedikter, B. J., Heinzmann, A., Vasina, E. M., Henskens, Y., et al. (2017). Platelet extracellular vesicles induce a pro-inflammatory smooth muscle cell phenotype. *Journal of extracellular vesicles*. doi:10.1080/20013078.2017.1322454

Valadi, H., Ekström, K., Bossios, A., Sjöstrand, M., Lee, J. (2007). Exosome-mediated transfer of mRNAs and microRNAs is a novel mechanism of genetic exchange between cells. *Nature Cell Biology* 9, 654–659

van der Zee, P., Biró, É., Ko, Y., de Winter, R., Hack, C. et al. (2006). P-Selectin- and CD63-Exposing Platelet Microparticles Reflect Platelet Activation in Peripheral Arterial Disease and Myocardial Infarction. *Clinical Chemistry*, doi: 10.1373/clinchem.2005.057414

Van Niel, G., D'Angelo, G. and Raposo, G. (2018). Shedding light on the cell biology of extracellular vesicles. *Nature Reviews Molecular Cell Biology*, doi: 10.1038/nrm.2017.125

Wachowicz, B., Morel, A., Miller, E., & Saluk, J. (2016). The physiology of blood platelets and changes of their biological activities in multiple sclerosis. *Acta neurobiologiae experimentalis* 76, 269-281.

Wang, L., Bi, Y., Yu, M., Li, T., Tong, D. (2018). Phosphatidylserine-exposing blood cells and microparticles induce procoagulant activity in non-valvular atrial fibrillation. *International Journal of Cardiology*, doi: 10.1016/j.ijcard.2018.01.116

Warren BA., Vales O. (1972). The release of vesicles from platelets following adhesion to vessel walls in vitro. *Brittish Journal Experimental Pathology* 53, 206-2015

Wieckowski, E., Visus, C., Szajnik, M., Szczepanski, M., Storkus, W., Whiteside, T. (2009). Tumor-derived microvesicles promote regulatory T cell expansion and induce apoptosis in tumor-reactive activated CD8 + T lymphocytes. *Journal of Immunology* 183, 3720-3730.

Willekens, F., Werre, J., Kruijt, J., Roerdinkholder-Stoelwinder, B., Groenen-Dopp, Y., et al. (2005). Liver Kupffer cells rapidly remove red blood cell-derived vesicles from the circulation by scavenger receptors. *Blood* 105, 2141–2145

Willms, E., Johansson, H., Mäger, I., Lee, Y., Blomberg, K. (2016). Cells release subpopulations of exosomes with distinct molecular and biological properties. *Scientific reports*, doi: 10.1038/srep22519

Witwer, K. W., Soekmadji, C., Hill, A. F., Wauben, M. H., Buzás, E. I., et al. (2017). Updating the MISEV minimal requirements for extracellular vesicle studies: building bridges to reproducibility. *Journal of extracellular vesicles*, doi:10.1080/20013078.2017.1396823

Wolf, P. (1967), The Nature and Significance of Platelet Products in Human Plasma. *British Journal of Haematology*, doi:10.1111/j.1365-2141.1967.tb08741.x

Wurzelmann M, Romeika J, Sun D. (2017). Therapeutic potential of brain-derived neurotrophic factor (BDNF) and a small molecular mimics of BDNF for traumatic brain injury. *Neural Regeneration Research*. doi: 10.4103/1673-5374.198964.

Yadav, S. and Storrie, B. (2016). The cellular basis of platelet secretion: Emerging structure/function relationships. *Platelets*, 28, 108-118.

Yáñez-Mó, M., Siljander, P.R., Andreu, Z., Zavec, A.B., Borràs, F.E., et al. (2015). Biological properties of extracellular vesicles and their physiological functions. *Journal Of Extracellular Vesicles*, doi: 10.3402/jev.v4.27066

Yang, Z. F., Ho, D. W., Lau, C. K., Tam, K. H., Lam, C. T., et al. (2006). Significance of the serum brain-derived neurotrophic factor and platelets in hepatocellular carcinoma. *Oncology Reports*, doi: 10.3892/or.16.6.1237

Zaldivia, M., McFadyen, J., Lim, B., Wang, X., Peter, K. (2017). Platelet-Derived Microvesicles in Cardiovascular Diseases. *Frontiers in Cardiovascular Medicine*, doi: 10.3389/fcvm.2017.00074

Zamora, C., Cantó, E., Nieto, J., Bardina, J., Cesar Diaz-Torné, C. et al. (2017). Binding of Platelets to Lymphocytes: A Potential Anti-Inflammatory Therapy in Rheumatoid Arthritis. *Journal of Immunology*, doi: 10.4049/jimmunol.1601708

Żmigrodzka, M., Guzera, M., Miśkiewicz, A., Jagielski, D., Winnicka, A. (2016) The biology of extracellular vesicles with focus on platelet microparticles and their role in cancer development and progression. *Tumour Biology*. doi: 10.1007/s13277-016-5358-6.

Xu, X. R., Carrim, N., Neves, M. A., McKeown, T., Stratton, T. W., et al. (2016a). Platelets and platelet adhesion molecules: novel mechanisms of thrombosis and anti-thrombotic therapies. *Thrombosis journal*, 14(Suppl 1), 29. doi:10.1186/s12959-016-0100-6

Xu, X.R., Zhang, D., Oswald, B., Carrim, N., Wang, X., et al. (2016b) Platelets are versatile cells: New discoveries in hemostasis, thrombosis, immune responses, tumor metastasis and beyond, *Critical Reviews in Clinical Laboratory Sciences* 53, 409-430

Nothing in life is to be feared, it is only to be understood. Now is the time to understand more, so that we may fear less.

— Marie Curie